symmetry

IMPACT FACTOR 2.7

CITESCORE 4.9

Article

A Study on the Various Aspects of Bounce Realisation for Some Choices of Scale Factors

Sanghati Saha, Ertan Güdekli and Surajit Chattopadhyay

Special Issue
Symmetry: Feature Papers 2023

Edited by
Prof. Dr. Sergei D. Odintsov

MDPI

https://doi.org/10.3390/sym15071332

symmetry

MDPI

Article

A Study on the Various Aspects of Bounce Realisation for Some Choices of Scale Factors

Sanghati Saha [1,†], Ertan Güdekli [2,†] and Surajit Chattopadhyay [1,*,†,‡]

[1] Department of Mathematics, Amity University, Kolkata, New Town, Rajarhat, Kolkata 700135, India; sanghati.saha2@s.amity.edu
[2] Department of Physics, Istanbul University, Istanbul 34134, Turkey; gudekli@istanbul.edu.tr
* Correspondence: schattopadhyay1@kol.amity.edu; Tel.: +91-824-038-4649
† These authors contributed equally to this work.
‡ Visiting Associate of the Inter-University Centre for Astronomy and Astrophysics (IUCAA), Pune, India.

Abstract: The current study examines the realisation of cosmic bounce in two situations involving two distinct scale factor selections, one of which is a scale factor already developed for bouncing and the other of which is a scale factor created by truncating a series expansion of a de Sitter scale factor. Generalized Chaplygin gas (GCG) is assumed to be the background fluid in both situations. When the scale factor is set to the first kind, the pre-bounce scenario's GCG energy density decreases due to contraction, reaches its lowest point at $t = 0$ during the bounce, and then rises as a result of expansion following the bounce. However, it is noted that the truncation has an impact on the density evolution from pre-bounce in the other scale factor scenario. The influence of bulk viscosity is shown in all circumstances, in addition to the influence of non-viscosity, and the test for stability makes use of the squared speed of sound. At the turn-around places, the null energy criterion is also violated. The final stage of the study includes a cosmographic analysis and a demonstration of the Hubble flow dynamics. In conclusion, we find that inflationary cosmology can also be realized with GCG as the background fluid for two-scale factor options. When the equivalent cosmic parameter is examined for pre-bounce and post-bounce scenarios, a symmetry is frequently seen. The symmetry occurs near the point of bouncing or turning.

Keywords: Generelized Chaplygin gas; scale factor; bounce cosmology; bulk viscosity

Citation: Saha, S.; Güdekli, E.; Chattopadhyay, S. A Study on the Various Aspects of Bounce Realisation for Some Choices of Scale Factors. *Symmetry* **2023**, *15*, 1332. https://doi.org/10.3390/sym15071332

Academic Editor: Sergei D. Odintsov

Received: 1 June 2023
Revised: 16 June 2023
Accepted: 20 June 2023
Published: 29 June 2023

1. Introduction

The evolution of the universe may or may not adhere to the conventional inflationary paradigm, which is a natural question for modern cosmology. An initial singularity is necessary for standard inflation to proceed. If this is not present, cosmic bounce is taken into account, in which case no initial singularity is present [1]. We have an alternative to the Big Bang cosmology in the form of big bounce scenarios. In [1], a bounce cosmology with modified gravity was demonstrated. It was found that the bouncing point is distinguished by a type IV singularity. In the models of a bouncing universe, the Big Bang is replaced by a bounce, releasing the Universe from a primordial singularity. It is well-known that bounce cosmologies are alternatives to the prevalent inflationary cosmology [2]. Holographic dark energy theory is among the intriguing possibilities for late-time acceleration. Although there has been much research on the holographic principle's late-time applications, specifically in the dark energy age, there has not previously been much work on implementing it. Reference [3] took steps forward in this approach in a trailblazing effort and created an inflationary realization of holographic origin. Inspired by the work of [4], the current study focuses on bounce realization in the presence of a version of Chaplygin gas. We will implement bounce cosmology through a model that is more frequently used to describe the late-time acceleration of the universe, so before moving on to the problems with the bounce scenario, let us take a look at the literature on the late-time acceleration of the universe.

One of the most important questions in the context of cosmic expansion is regarding acceleration. Ia supernovae (SNe Ia) [5], the cosmic microwave background (CMB) [6], the Wilkinson microwave anisotropy probe (WMAP) [7–11], and large-scale redshift survey structures (LSS) [12–16] are just a few of the many observational studies of the cosmic universe that demonstrate that the universe is currently expanding at an accelerated rate [17]. Although the CMB is isotropic, the universe may not be homogeneous if our place in the universe is unique. These cosmological models were built using spherically symmetric models with our location close to the symmetric center [18].

The phrase "dark energy" (DE) refers to a fictitious fluid with negative pressure driving the universe's fast expansion. This gravitationally repellent exotic energy exerts an equation of state (EoS)-parameter-driven repulsion. The EoS parameter is given by $w = \frac{p}{\rho} < -1/3$, where p denotes the thermodynamic pressure and ρ denotes the energy density. This mysterious cosmic fluid makes up nearly three-fourths of the universe's entire mass–energy density [19]. It is invisible, just as dark matter is. Astrophysical observations between cosmic entities can reveal it. DE remains an unknown form of energy. DE, as a form of exotic energy, is included in the stress–energy–momentum tensor of the field equations in Einstein's theory of general relativity. There is a direct correlation between the universe's matter–energy and the universe's global or local geometry in the general theory of relativity (GTR) [20,21]. DE can be identified by altering the rate at which the cosmos expands and the rate at which galaxies and gravitationally bound groupings of galaxies form due to gravitational perturbations [22]. The earliest dark energy theory states that a fundamental energy density is inherent to vacuum energy [23], a key component of Einstein's cosmological constant [24,25]. Reference [26] observed a method of vacuum energy's regularization. The importance of radiative instability and Weinberg's no-go theorem is highlighted in [27,28] to emphasize the problem's global aspect. This lecture series introduces the specified sequestration, a novel representational strategy for the cosmological constant problem that integrates renormalization and general relativity by canceling the vacuum energy of the standard model. Dark energy may be considered in two different contexts in general. They are the static and dynamic dark energy models, respectively. The first static dark energy model is the positive cosmological constant model. However, this static model was unable to explain the current temporal vacuum energy ambiguity (cosmic coincidence problem). This is why dynamical dark energy theories were proposed. The simplest candidate of DE is Einstein's cosmological term symbolized as Λ with $\omega_\Lambda = -1$ [28–31], introduced by Albert Einstein to augment his field equations of the general theory of relativity. Numerous dark energy models having time-varying EoS parameters supported by observations, such as quintessence [32–34], phantom [35–39], quintom [40–45], tachyon fieldd [46–48], hessence [49,50], k-essence [51], Chaplygin gas [52–56], and holographic dark energy [57–61], have been presented to identify the cause behind the cosmic accelerated expansion. Broader pictures of the various facets of DE in the form of a review is available in the [61–70].

Unified dark energy (UDE) models are especially intriguing in this aspect, as they have the benefit of simulating both DM and DE features with a single underlying fluid. The Chaplygin gas (CG) [71–73] was the first UDE prototype, often characterized as a perfect fluid with an equation of state given by $p = -\frac{A}{\rho}$ with $A > 0$. The equation of state (EoS) parameter of the CG interpolates from $\omega = 0$ at early periods to $\omega = 1$ at late times when the CG energy density achieves a minimal value. This model piqued people's curiosity because of its relationship to string theory d-branes. One of the numerous potential sources of dark energy is Chaplain gas, which can combine cold dark matter (CDM) [74–76], another dark component of the universe with DE. Additionally, the equation of state specifies this as a perfect fluid used to explain idealized distributions of matter in general relativity. The CG model was later generalized to incorporate an additional parameter α with EoS,

$$p = -\frac{A}{\rho^\alpha} \ . \tag{1}$$

This Equation (1) non-homogeneous Chaplygin gas provides a complete, reasonable argument for linking DE and DM's numerous functions. This odd fluid demonstrates the most basic deformations of the most common ΛCDM models. It was first recommended that $\alpha = 1$. Following that, it was argued that $\alpha \neq 1$, conforming to the general result. Sergey Chaplygin developed this equation of state as a useful mathematical approximation for determining the aerodynamical lifting force on an aeroplane wing. This isentropic fluid is only supersymmetrically generalizable. Chaplygin gas is crucial to the narrative of string theory. The most important aspect of Chaplygin gas is that it can depict a transition from decelerated cosmic expansion to the current stage of cosmic acceleration, and as a single component, it can unify dark matter and dark energy, which together comprise the universe's dark sector. This non-homogeneous Chaplygin gas gives a wide plausible explanation for the various functions of DE and DM. This unusual fluid exhibits the simplest deformations of the most common ΛCDM models. M.C. Bento introduced the generalized Chaplygin gas (CGC) [77–79] model during the beginning of the twenty-first century, with $A > 0$ and $0 \leq \alpha \leq 1$ with the equation of state seen in Equation (1). Various models of Chaplygin gas [80–88] may easily interpolate between a non-relativistic matter phase with vanishing pressure $(p = 0)$ and a negative-pressure period dominated by DE.

It is crucial to highlight that this late-time acceleration is by no means the only accelerated period of the cosmos. Instead, we may conclude that our contemporary universe is experiencing an accelerated expansion based on observational investigations. The inflationary phase is another stage of this expansion in the initial stages. Several inconsistencies in the big bang cosmology were afterward transmitted in the works of [89,90] within the context of the inflationary cosmology, which is representative of the early cosmos. In [91,92], it was demonstrated how cosmic acceleration and early inflation can work together. Although the so-called "standard model of the universe" still retains the initial singularity issue, inflation is now thought to have played a substantial role in the cosmic history of the universe. A singularity is inevitable if inflation is accomplished using a scalar field and the background space–time exhibits a typical Einstein action. As a result, a great deal of effort has been put into finding a solution to this problem using methods such as effective field theory or quantum gravity effects that breach the null energy requirement (also known as "island cosmology models"). The issue of cosmic singularity may have an answer in non-singular bouncing cosmologies. Cosmic bounce hypotheses provide a distinct viewpoint on the early cosmos [92–95].

The idea of re-expanding a closed universe that had previously collapsed to a highly dense state was first put forth by Tolman in the 1930s. Since then, other bouncing models have been proposed to offer a convincing explanation for the origin of our universe. The key benefit of bouncing cosmology is that it provides a solution to the singularity issue that plagues the dominant cosmological paradigm [96,97]. The Big Bounce (a seamless transition from contraction to expansion) takes the place of the singularity of the Big Bang. Bounce cosmology enables a more comprehensive view of the early cosmos in this way. This offered a non-phantom standard cosmology that illustrated the transition from the pre-inflationary to the inflationary period and recovered the recently discovered dark energy era. Whether the universe expanded following the Big Bang singularity or resulted from a non-singular bounce scenario is debated among contemporary cosmologists. One cosmological explanation for the early universe is inflation, which offers a potential solution to the horizon and flatness issues. Additionally, it forecasts a power spectrum of curvature perturbations that is almost scale-invariant.

Going further back in time, the inflationary scenario produces the Big Bang singularity, an initial cosmic singularity in which geodesic incompleteness creates a space–time curvature singularity. An alternative to inflation is bouncing cosmology, which can produce a curvature power spectrum invariant with regard to scale, and the bouncing scenario leads to the evolution of the universe with no singularity [96–102]. When the contraction in the matter bounce scenario begins, the cosmos goes through a period in which matter dominates. Furthermore, a bounce occurs in the absence of a singularity. In other words, it

indicates that the universe transitioned smoothly from an accelerated collapse phase to an expanding age. Following the bounce, the universe entered a phase of matter-dominated expansion. Numerous varieties of finite-time singularities in cosmology, other than the Big Bang singularity, are addressed in [103]. The worst of them all is the Big Rip or Type I singularity. Finite temporal singularities of Type II, III, and IV are equivalent. In the case of a Type I, II, or III singularity, the universe's effective energy density and/or effective pressure diverge at the point of singularity. In contrast, the effective energy density and effective pressure of the universe remain finite during the instance of singularity in the Type IV singularity, making the Type IV singularity the milder of the finite time singularities. Specifically, unlike the Big Rip singularity, the Type IV singularity lacks geodesic incompleteness. As a result, the universe can easily pass through a Type IV singularity (if any), and the Type IV singularity does not cause catastrophic events to the observable quantities.

The four most fundamental energy states employed in GR are null, weak, strong, and dominant. The well-known Hawking–Penrose singularity refers to the strong energy condition (SEC), whose violation causes the observed rapid expansion. The null energy condition (NEC) is a prerequisite for proving the second law of black hole thermodynamics. For singularity theorems, they appear to rule out a bounce. It can be demonstrated that unless matter violates the null energy condition (NEC), a spatially flat, homogeneous, and isotropic space–time cannot experience a nonsingular bounce. There are some intriguing NEC-violating hypotheses that might result in a bounce or other "restart" of the cosmos. However, breaking the NEC without causing severe short-distance instability is challenging. In compact dimensions, known stable sources such as orientifolds and Casimir energy densities break the NEC. In an accelerating universe (either during primordial inflation or the current dark energy dominance), the NEC violation from these sources is a crucial component in stabilising Ricci flat extra dimensions (such as Calabi–Yau compactifications). However, because the volume of the compact space is inversely proportional to the NEC violation from these sources, they cannot be employed to initiate bounces in a noncompact/large universe.

The rest of the paper is organized as follows. In Section 2, we demonstrate bounce realization with Chaplygin gas. In Section 3, the bounce cosmology with respect to an e-folding number is demonstrated. The violation of the null energy condition is tested in Section 4. A cosmographic analysis is carried out in Section 5. In Section 6, we discuss the Hubble flow dynamics. Inflation via a scalar field is discussed in Section 7. The work is concluded in Section 8.

2. Bounce Realization with Chaplygin Gas

This section is devoted to the discussion of the realization of cosmological bounce with Chaplygin gas. In this context, let us mention that the study of cosmological bounce in the presence of Chaplygin gas is not new. Earlier, Salehi [4] discussed a realization of cosmological bounce in the presence of an extended Chaplygin gas model with an EoS as $p = A\rho - \frac{B}{\rho^{\alpha}}$ and found solutions for a singularity-free cosmological model through a cyclic universe with the minimal and maximal values of the scale factor. In another study, Chattopadhyay [100] demonstrated a detailed account of the possibility of the realization of cosmological bounce in the presence of modified Chaplygin gas. Pourhassan [104] discussed the unification of early inflationary expansion with late-time acceleration through Chaplygin gas cosmology. A survey of these studies motivated us to work on the possibility of bounce realization with different versions of scale factors and in the presence of bulk viscous pressure. In the context of the work to be reported in the subsequent sections, we would like to mention that the bouncing cosmology provides an alternative to traditional expanding cosmologies by avoiding an initial singularity. The cosmos expands once more after a brief period of constriction due to the cost, which is brought on by speculation about some hypothetical new physics at the bounce. Since viscosity is typically simply parametrized in physically driven situations, it is still unclear if isotropization may genuinely occur in these situations. Even though viscosity coefficients have a long history

in cosmology, their physical relevance has traditionally been regarded as minor, if not subdominant. Viscosity is believed to have the largest impact during neutrino decoupling in theories of the very early cosmos [105]. The singularity problem of the conventional Big Bang cosmology may be resolved by a bouncing universe, which first contracts to a non-vanishing minimum radius before expanding. It can be demonstrated that after a successful bounce, the null energy condition (NEC) is broken for a while in the context of the typical 4-dimensional Friedmann-Robertson-Walker (FRW) cosmology with Einstein gravity. Additionally, the Equation of state(EoS) parameter of the universe's matter content ω must change from $\omega < -1$ to $\omega > -1$ in order for the universe to enter the hot Big Bang epoch following the bouncing [106–108]. Today's late-time accelerating and the early-time inflation are generally acknowledged as two accelerated epochs in the development of the cosmos. These two accelerating periods' strong resemblances suggest that the same basic event is responsible for their beginning [109–135]. To start with, we have considered two bouncing scale factors from the [136,137]. In [136], the authors looked at how $f(T)$ gravity may be used to realize the matter bounce cosmology. They recreated the particular form of $f(T)$ that creates an explicit scale-factor form that connects matter-like contraction and expansion through a smooth nonsingular bounce phase. They explored an alternate strategy to escape the Big Bang singularity encountered in the conventional inflationary cosmology using their study, which demonstrated the potential of integrating the $f(T)$ gravity and bounce cosmologies. Consider the nonsingular scale factor from [136],

$$a(t) = a_0\left(1 + \frac{3t^2\sigma}{2}\right)^{\frac{1}{3}} . \tag{2}$$

where a_0 is the scale factor at the bouncing point and σ is a positive parameter describing the speed with which the bounce occurs. Such a method demonstrates the bouncing behavior associated with matter-dominated contraction and expansion, as well as the advantage of allowing for semi-analytic solutions. In this case, t ranges between $-\infty$ and $+\infty$, with $t = 0$ serving as the bounce point.

Therefore, the equivalent Hubble parameter, whicht assesses how quickly the cosmos is expanding, is

$$H = \frac{t\sigma}{1 + \frac{3t^2\sigma}{2}} . \tag{3}$$

Let us talk about the scenario we provide in this paper, which is based on the idea that a de Sitter bounce occurred during the pre-inflationary period of the universe and that this was subsequently followed by a quasi-de Sitter era. In [137] the authors extracted the de Sitter scale factor solution,

$$a(t) = a_0 e^{H_0 t} . \tag{4}$$

with a_0 and H_0 as constants of integration. In this part, we have modified this scale factor Equation (4) for generating the bounce in more detail. It is well-known that the cosmic scale factor, which links comoving distances to distances at some reference time, is a time-dependent function that describes the universe's expansion. $a(t)$, which is equal to 1 at today's point, is the symbol for the cosmic scale factor. In the standard inflationary cosmology paradigm, the inflationary time is measured using a de Sitter or quasi-de Sitter development. We must always ensure that the inflationary period is long enough to allow for the resolution of any issues with the cosmology of the traditional Big Bang hypothesis. Equation (4) can be written as using the expansion of the function e^x

$$a(t) = a_0\left(1 + H_0 t + \frac{H_0^2 t^2}{2!} + \frac{H_0^3 t^3}{3!} + \frac{H_0^4 t^4}{4!} + \frac{H_0^5 t^5}{5!} + \frac{H_0^6 t^6}{6!} + ...\right). \tag{5}$$

Here, we have considered two cases:

Case-1

Here, we have considered expansion of scale factor Equation (5) upto $4rth$ order of cosmic time t.

$$a(t) = a_0\left(1 + H_0 t + \frac{H_0^2 t^2}{2!} + \frac{H_0^3 t^3}{3!} + \frac{H_0^4 t^4}{4!}\right). \tag{6}$$

by taking assumption $H_0 < 2.5$.

Therefore, the Hubble parameter is

$$H = \frac{4H_0\left(6 + 6H_0 t + 3{H_0}^2 t^2 + {H_0}^3 t^3\right)}{24 + 24H_0 t + 12{H_0}^2 t^2 + 4{H_0}^3 t^3 + {H_0}^4 t^4} \ . \tag{7}$$

Case-2

Now, we have taken expansion of scale factor Equation (5) upto $5th$ order of cosmic time t.

$$a(t) = a_0\left(1 + H_0 t + \frac{H_0^2 t^2}{2!} + \frac{H_0^3 t^3}{3!} + \frac{H_0^4 t^4}{4!} + \frac{H_0^5 t^5}{5!}\right). \tag{8}$$

by taking assumption $H_0 < 3$.

Then,

$$H = \frac{5H_0\left(24 + 24H_0 t + 12{H_0}^2 t^2 + 4{H_0}^3 t^3 + {H_0}^4 t^4\right)}{120 + 120H_0 t + 60{H_0}^2 t^2 + 20{H_0}^3 t^3 + 5{H_0}^4 t^4 + {H_0}^5 t^5} \tag{9}$$

Here, we have plotted three Hubble parameters and shown their bounce cosmology in Figure 1. In the first two cases, $H < 0$ is the pre-bounce scenario, $H = 0$ is the bouncing point, and $H > 0$ is the post-bounce scenario. We would like to mention that in all the plots, the unit of cosmic time t is Gyr, and the unit of dark energy density is J/m^3.

As anticipated, given the bouncing behavior, the Hubble parameter expands from the early cosmos and disappears at the epoch $t = 0$ before continuing to rise (Figure 1 (left panel)). In Figure 1 (middle panel), there is also a non-singular bounce, although in Figure 1 (right panel), we can see a bounce singularity. In this study, we have compared nonsingular bounce cosmologies by taking bouncing scale factors from Equation (2) and from a modified Equation (6) with a background fluid consisting of a generalized Chaplygin gas (GCG).

Now, we have considered the background evolution fluid as a barotropic GCG whose equation of state (EoS) [138] is

$$P = \frac{-B}{\rho^{\alpha}}, \tag{10}$$

where we have denoted thermodynamic pressure as P and total energy density as ρ; and B is a positive constant, and α lies between 0 and 1. The GCG model may be used to explain both the development of the energy density perturbation and the rapid growth of a late epoch. This unification is driven by Equation (10), the equation of state of the background fluid. We assume that dark energy and dark matter constitute the totality of the universe throughout this work, while dark matter under no pressure leads to $P_m = 0$. In doing so, we have overlooked the contributions of other components. In a Friedmann–Robertson–Walker (FRW) universe dominated by bulk viscous fluid, the Friedmann's field equations [138] are

$$\frac{6\ddot{a}}{a} = -(\rho + 3(P + \Pi)) \ , \tag{11}$$

and

$$3H^2 = \rho_{Total} \ , \tag{12}$$

where, Π be the bulk viscous pressure of background evolution of universe.

The early stage of the universe's expansion is thought to be driven by a viscous Chaplygin gas, with Pi being the bulk viscous pressure and Π being given by $\Pi = -3H\xi$, where ξ is a function of the Hubble parameter. Using the conservation equation for pressureless dark matter once more, we can see that

$$\dot{\rho_m} + 3H\rho_m = 0 \ . \tag{13}$$

$$Or, \ \rho_m = \rho_{m0} a(t)^{-3} \ . \tag{14}$$

where, ρ_m be the dark matter density.

We derive the Hubble parameters of Equations (3) and (7) from the scale factors in Equations (2) and (6), respectively.

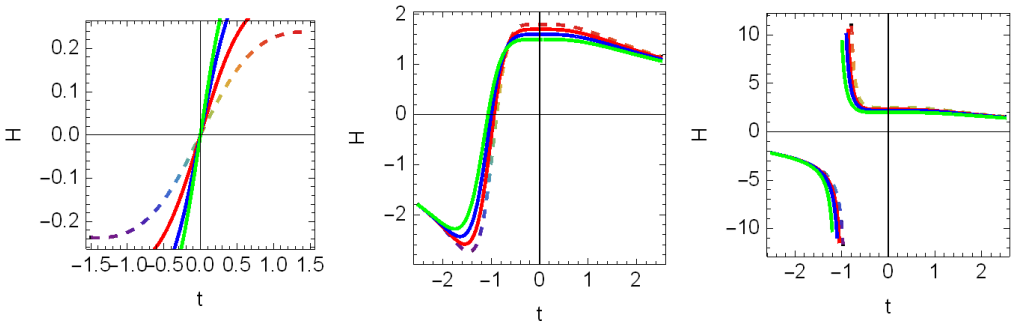

Figure 1. Behavior of Hubble parameters for the scale factors in Equation (2) (**left** panel), Equation (6) (**middle** panel), and Equation (8) (**right** panel) with $\sigma = (0.34, 0.56, 0.86, 1.12)$, $\rho_{m0} = 0.32$, $a_0 = 10.6$, and $H_0 = (1.8, 1.7, 1.6, 1.5)$ for the lines coloured in Rainbow, Red, Blue, Green respectively.

2.1. Bouncing Model-I

In this subsection, we report a special case study by taking the bouncing scale factor from Equation (2), where the background fluid is GCG. From Equation (12), we can obtain the total density of background fluid as

$$\rho_{Total} = \frac{12t^2\sigma^2}{(2+3t^2\sigma)^2} \tag{15}$$

Therefore, expression of thermodynamic pressure will be as follows:

$$P = -12^{-\alpha} B \left(\frac{t^2\sigma^2}{(2+3t^2\sigma)^2} \right)^{-\alpha} \ . \tag{16}$$

Here, we have found that in the pre-bounce scenario, the GCG energy density in Figure 2 (left panel) reduces owing to contraction, reaches its lowest point at $t = 0$ during the bounce, and increases after the bounce because of expansion. This illustration shows a fast rise in density caused by inflation, followed by a stability of density throughout later periods of the cosmos, which is consistent with the inflationary theory of the universe. The symmetry of the plots around the bouncing point is due to the presence of t^2 in the related expressions. Because of t^2, the plots have symmetry around the bouncing point. The continuous and controlled background development of the energy density is present.Confirmed At $t = 0$, the bounce is very noticeable. Thermodynamic pressure in Figure 3 (right panel), which is negative pressure, supports the dark energy era in addition to GCG as background fluid. Therefore, from the equation of state parameter $\omega = \frac{P}{\rho}$, we obtain

$$\omega = -12^{-1-\alpha} B \left(\frac{t^2\sigma^2}{(2+3t^2\sigma)^2} \right)^{-1-\alpha} \ . \tag{17}$$

From Equations (11), (15), and (16), we obtain the bulk viscous pressure,

$$\Pi = \frac{12^{-\alpha}\left(\frac{t^2\sigma^2}{(2+3t^2\sigma)^2}\right)^{1-\alpha}\left(-2^{3+2\alpha}3^{\alpha}\sigma\left(\frac{t^2\sigma^2}{(2+3t^2\sigma)^2}\right)^{\alpha}+B\left(2+3t^2\sigma\right)^2\right)}{t^2\sigma^2}. \tag{18}$$

Therefore, we can obtain an effective EoS parameter by $\omega_{eff} = \frac{P+\Pi}{\rho}$, and from $\Pi = -3H\xi$, we can derive the viscosity coefficient Ξ as

$$\xi = \frac{8 - 12^{-\alpha}Bt^2\sigma\left(\frac{t^2\sigma^2}{(2+3t^2\sigma)^2}\right)^{-1-\alpha}}{6t(2+3t^2\sigma)}. \tag{19}$$

We have plotted the bulk viscous pressure and viscosity coefficient in Figure 3. The pre-bounce contraction stage comes first. The bulk viscous pressure is negative in the pre-bounce scenario, but the viscosity coefficient ξ also appears to be negative, as shown in the left panel of Figure 3. This is in contrast to what occurs in the post-bounce scenario, where ξ must be unavoidably positive to maintain the bulk viscous pressure Π as negative. It should be noticed that H is negative during the pre-bounce contracting phase. Thus, $\Pi = -3H\xi < 0$ holds true if ξ is negative. Therefore, the negative sign of ξ in the pre-bounce situation is compatible with $\Pi < 0$. Further analysis reveals that the effects of bulk viscosity gradually increase during post-bounce expansion and gradually decrease during contraction. Once more, it is clear that the denominator of this equation, Equation (15), reaches zero at the point of bouncing, $t = 0$. The growth of the reconstructed EoS parameter (left panel) diverges as a result, as seen in Figure 4. The EoS parameter crosses the phantom border both before and after the bounce. In spite of its effectiveness, the EoS parameter (right panel) avoids the Big Rip singularity in the post-bounce scenario.

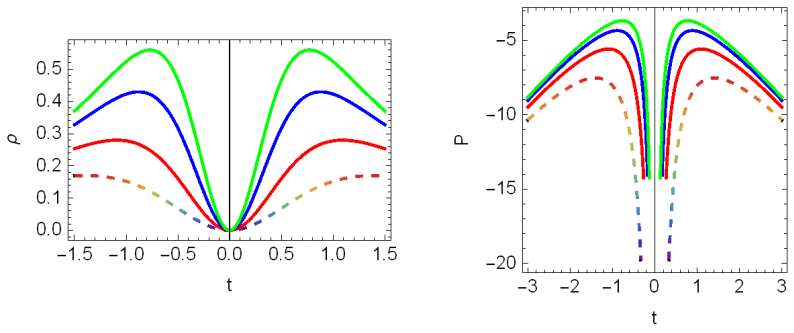

Figure 2. Evolution of reconstructed energy density (**left** panel) and thermodynamic pressure (**right** panel) for bouncing model I with $\sigma = (0.34, 0.56, 0.86, 1.12)$, $\rho_{m0} = 0.32$, $a_0 = 10.6$, $\alpha = 0.6$ for the lines coloured in Rainbow, Red, Blue, Green respectively.

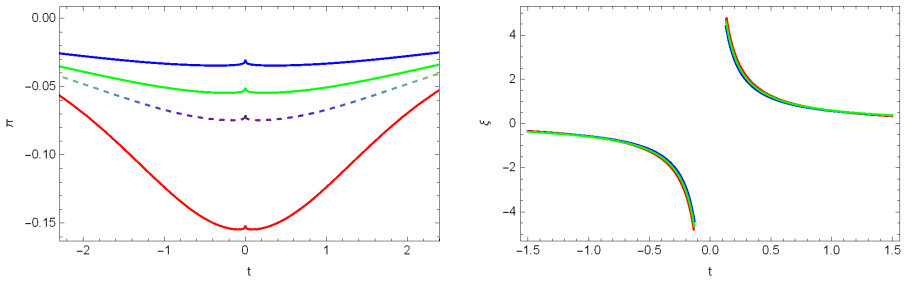

Figure 3. Evolution of the reconstructed bulk viscous pressure Π in the (**left** panel) and evolution of the bulk viscosity co-efficient ξ in the (**right** panel) for bouncing model I with $\sigma = (0.34, 0.56, 0.86, 1.12)$, $\rho_{m0} = 0.32$, $a_0 = 10.6$, $\alpha = 0.6$ for the lines coloured in Rainbow, Red, Blue, Green respectively.

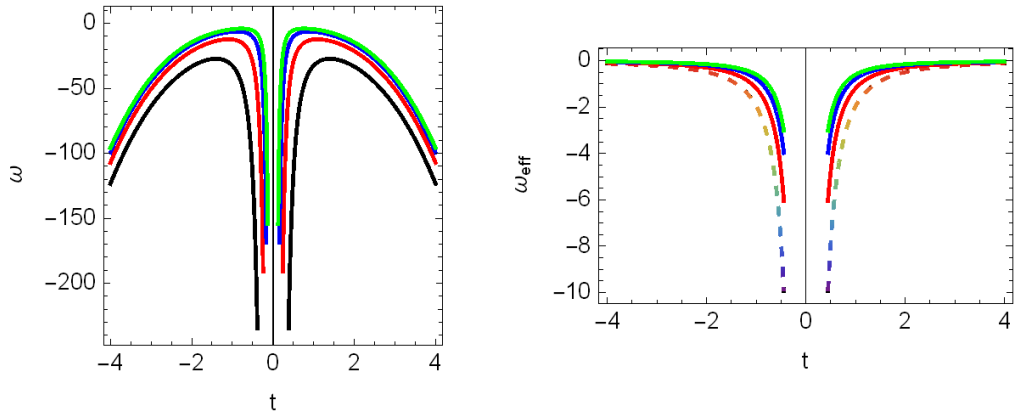

Figure 4. Behavior of reconstructed EoS parameter in (**left** panel) and effective EoS parameter in (**right** panel) for bouncing model I with $\sigma = (0.34, 0.56, 0.86, 1.12)$, $\rho_{m0} = 0.32$, $a_0 = 10.6$, $\alpha = 0.6$ for the lines coloured in Green, Blue, Red, Black for (**left** panel) and Rainbow, Red, Blue, Green for (**right** panel) respectively.

Now we investigate the density parameter, Ω. The ratio of the observed (or real) density to the Friedmann universe's critical density is known as the density parameter. The cosmos is on the approach of reaching the critical density that would cause it to expand indefinitely, according to several studies that seek to explain the universe's rate of expansion. We portrayed density as a fraction of the density required for this critical condition in order to investigate the universe's expansion in a novel manner. In order to prove that dark energy rules our universe throughout this epoch of expansion, we looked at fractional densities. It is believed that the Big Bang's early history was initially dominated by radiation, then by matter, and that dark energy presently has the most effect. Let us define the fractional densities [139]

$$\Omega_{Energy} = \frac{1}{3H^2}\rho_{Energy}. \tag{20}$$

$$\Omega_{Matter} = \frac{1}{3H^2}\rho_{Matter}. \tag{21}$$

Here,

$$\Omega_{Energy} + \Omega_{Matter} = 1. \tag{22}$$

Therefore, for this case,

$$\Omega_{Matter} = \frac{\rho_{m_0}(2 + 3t^2\sigma)}{12t^2\sigma^2}. \tag{23}$$

$$\Omega_{Energy} = 1 - \Omega_{Matter}. \tag{24}$$

We have carried out a stability analysis using the square of the speed of sound [140] in the framework of Einstein's gravity.

$$V_s^2 = \frac{dp}{d\rho}. \tag{25}$$

The model's stability is determined by $V_s^2 \geq 0$. If the value is negative, it indicates that the model is unstable. We have included the squared speed of sound below for GCG reconstruction schemes in Einstein's framework for the bouncing scale factor in Equation (2) and plotted V_s^2 versus cosmic time t.

It is evident from the plot of the reconstructed fractional densities over cosmic time t in Figure 5 (left panel) that the universe is changing from a structure that is dominated by matter to a structure that is dominated by energy. With the help of the GCG background

evolution fluid, the aforementioned graphic shows that dark matter is becoming weaker over time, while dark energy is becoming stronger. In the framework of Einstein's theory of gravity, the square speed of sound Figure 5 (right panel) diverges at the bouncing point for the model I. This suggests that the model may be unstable at the bouncing point and calls for more research.

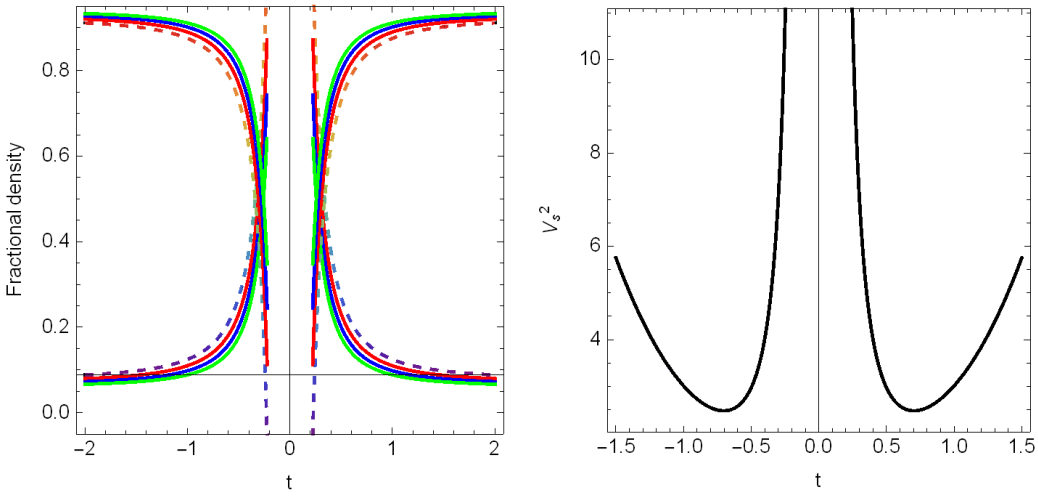

Figure 5. Evolution of fractional density (**left** panel) with $\sigma = (0.34, 0.56, 0.86, 1.12)$, $\rho_{m0} = 0.32$, $a_0 = 10.6$, $\alpha = 0.6$ for the lines coloured in Rainbow, Red, Blue, Green respectively and stability analysis (**right** panel) with $\sigma = (0.34, 0.56, 0.86, 1.12)$, $\rho_{m0} = 0.32$, $a_0 = 10.6$, $\alpha = 0.6$ for the overlapping lines coloured in Red, Green, Blue, Black for (**right** panel) for bouncing model I.

2.2. Bouncing Model II

In this part, we discuss a unique instance of the research using the bouncing Noijoiri–Odintsov scale factor from Equation (6), with the background fluid being GCG. We may obtain the total density of background fluid by using Equation (12).

$$\rho_{Total} = \frac{48{H_0}^2\left(6 + 6H_0t + 3{H_0}^2t^2 + {H_0}^3t^3\right)^2}{\left(24 + 24H_0t + 12{H_0}^2t^2 + 4{H_0}^3t^3 + {H_0}^4t^4\right)^2}. \tag{26}$$

Therefore, the thermodynamic pressure is

$$P = -48^{-\alpha}B\left(\frac{{H_0}^2\left(6 + 6H_0t + 3{H_0}^2t^2 + {H_0}^3t^3\right)^2}{\left(24 + 24H_0t + 12{H_0}^2t^2 + 4{H_0}^3t^3 + {H_0}^4t^4\right)^2}\right)^{-\alpha}. \tag{27}$$

We have plotted energy density and thermodynamic pressure with respect to cosmic time t in the following Figure 6 (left panel) and Figure 6 (right panel) respectively. In order to maintain a positive energy density (left panel) throughout the entire process, the minimal matter geometry coupling scale factor parameter H_0 should be restricted to a positive value that is less than 2.5. We discovered that in the pre-bounce scenario, the GCG energy density reduces owing to contraction, reaches its lowest value at the bouncing point, and increases due to expansion after the bounce. Since it does not depict a sudden increase in density brought on by inflation but rather a progressive stabilization of energy density over time, this image does not support the inflationary expansion of the cosmos. Negative thermodynamic pressure supports the model's input from dark energy Figure 6 (right panel).

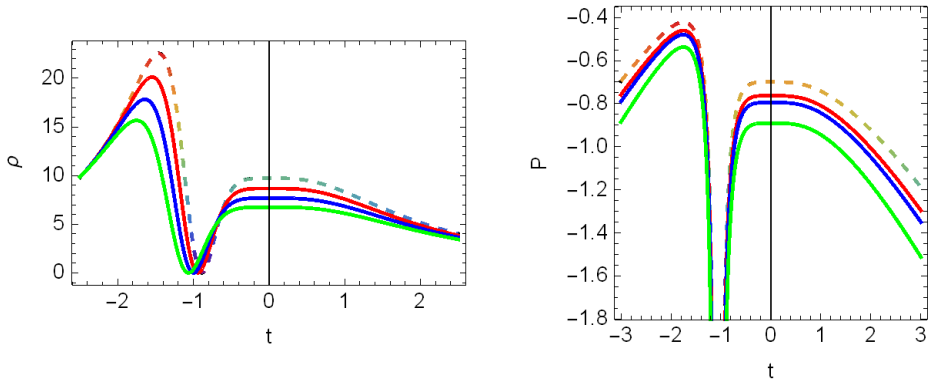

Figure 6. Evolution of reconstructed energy density (**left** panel) and thermodynamic pressure (**right** panel) with $H_0 = (1.8, 1.7, 1.6, 1.5)$ for the lines coloured in Rainbow, Red, Blue, Green respectively for bouncing model II

The EoS parameter ω can be represented as

$$\omega = -48^{-1-\alpha} B \left(\frac{{H_0}^2 \left(6 + 6H_0 t + 3{H_0}^2 t^2 + {H_0}^3 t^3\right)^2}{\left(24 + 24H_0 t + 12{H_0}^2 t^2 + 4{H_0}^3 t^3 + {H_0}^4 t^4\right)^2} \right)^{-1-\alpha} \tag{28}$$

Therefore, the bulk viscous pressure is

$$\begin{aligned} \Pi = 48^{-\alpha} B \left(\frac{{H_0}^2 \left(6+6H_0 t+3{H_0}^2 t^2+{H_0}^3 t^3\right)^2}{\left(24+24H_0 t+12{H_0}^2 t^2+4{H_0}^3 t^3+{H_0}^4 t^4\right)^2} \right)^{-\alpha} \\ - \frac{16{H_0}^2 \left(6+6H_0 t+3{H_0}^2 t^2+{H_0}^3 t^3\right)^2}{\left(24+24H_0 t+12{H_0}^2 t^2+4{H_0}^3 t^3+{H_0}^4 t^4\right)^2} - \frac{8H_0 \left(6+6H_0 t+3{H_0}^2 t^2+{H_0}^3 t^3\right)}{24+24H_0 t+12{H_0}^2 t^2+4{H_0}^3 t^3+{H_0}^4 t^4} \end{aligned} \tag{29}$$

Furthermore, the derived effective EoS parameter ω_{eff} is

$$\omega_{eff} = -\frac{24+12{H_0}^2 t(1+t)+{H_0}^4 t^3(2+t)+12H_0(1+2t)+2{H_0}^3 t^2(3+2t)}{6H_0\left(6+6H_0 t+3{H_0}^2 t^2+{H_0}^3 t^3\right)} \tag{30}$$

Thus, we have the viscosity coefficient ξ,

$$\xi = \frac{X+Y}{Z}, \tag{31}$$

where $X = 192 + 96H_0 + 192H_0 t + 96{H_0}^2 t + 96{H_0}^2 t^2 + 48{H_0}^3 t^2 + 32{H_0}^3 t^3 + 16{H_0}^4 t^3 + 8{H_0}^4 t^4$,

$Y = -48^{-\alpha} B H_0 (6 + H_0 t(6 + H_0 t(3 + H_0 t)))\left(\frac{{H_0}^2 (6+H_0 t(6+H_0 t(3+H_0 t)))^2}{(24+H_0 t(24+H_0 t(12+H_0 t(4+H_0 t))))^2}\right)^{-1-\alpha}$,

and $Z = 12(24 + H_0 t(24 + H_0 t(12 + H_0 t(4 + H_0 t))))$.

It should be noted once more that the denominator of Equation (28) tends zero at the moment of bounce, $t \to 0$. This results in a diverging increase of the reconstructed EoS parameter (left panel), as seen in Figure 7. Both before and after the bounce, the EoS parameter crosses the phantom barrier. In Figure 7 (right panel) we have plotted effective EoS parameter. Now, we have represented reconstructed bulk-viscous pressure in Figure 8 (left panel) and bulk-viscous co-efficient in Figure 8 (right panel). In the early universe, the impact of bulk viscous pressure is negligible although according to further investigation, the impacts of bulk viscosity steadily grow during post-bounce expansion. The positive sign of ξ is therefore consistent with $\Pi < 0$ as $H > 0$ in the post-bounce scenario.

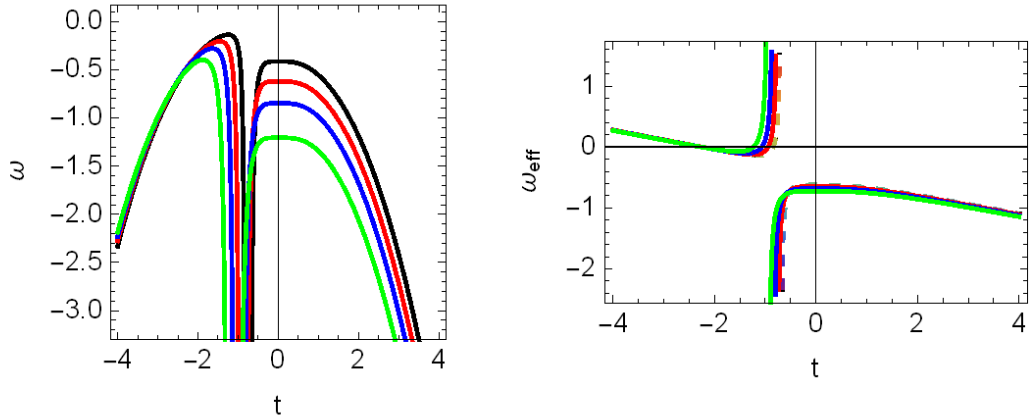

Figure 7. Behavior of reconstructed EoS parameter (**left** panel) with $H_0 = (2.3, 2.1, 1.9, 1.7)$ for the lines coloured in Black, Red, Blue, Green respectively and effective EoS parameter (**right** panel) with $H_0 = (1.8, 1.7, 1.6, 1.5)$ for the lines coloured in Rainbow, Red, Blue, Green respectively for bouncing model II.

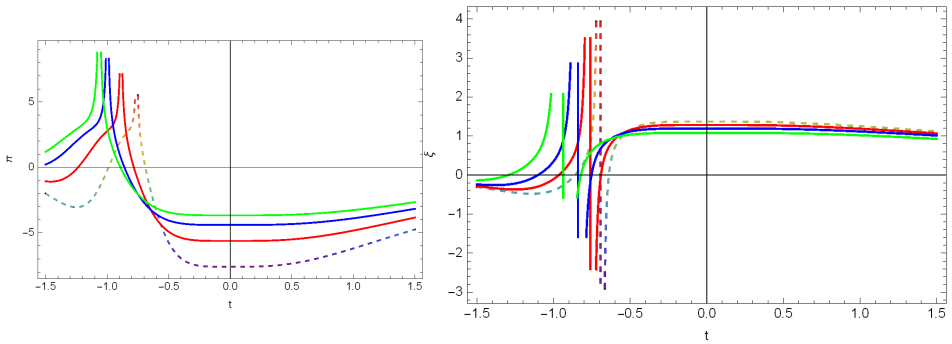

Figure 8. Evolution of the reconstructed bulk viscous pressure Π (**left** panel) and bulk viscosity co-efficient ξ (**right** panel) with $H_0 = (1.8, 1.7, 1.6, 1.5)$ for the lines coloured in Rainbow, Red, Blue, Green respectively for bouncing model II.

We have thus computed a reconstructed Ω_{Matter} and Ω_{Energy} for the scale factor from Equation (6) using Equations (26), (20), and (7), and this can be evaluated as follows:

$$\Omega_{Energy} = \frac{-288\rho_{m_0} + {a_0}^3{H_0}^2(6 + H_0t(6 + H_0t(3 + H_0t)))^2(24 + H_0t(24 + H_0t(12 + H_0t(4 + H_0t))))}{{a_0}^3{H_0}^2(6 + H_0t(6 + H_0t(3 + H_0t)))^2(24 + H_0t(24 + H_0t(12 + H_0t(4 + H_0t))))} \quad . \tag{32}$$

$$\Omega_{Matter} = 1 - \Omega_{Energy} \quad . \tag{33}$$

Now, utilizing the square speed of sound from Equation (25) in the context of Einstein's theory of gravity, we conduct a stability analysis. $V_s^2 \geq 0$ determines the stability of the model. A negative number suggests that the model is unstable. We have plotted V_s^2 with cosmic time t and added the squared speed of sound below for GCG reconstruction approaches in Einstein's framework for the bouncing scale factor from Equation (6). The plot of the reconstructed fractional densities over cosmic time t in Figure 9 (left panel) shows that the universe is transitioning from a structure that is dominated by matter to a structure that is dominated by energy. The aforementioned figure demonstrates that dark matter is weakening with time while dark energy is strengthening with the aid of the GCG background evolution fluid. In Figure 9 (right panel) $V_s^2 \geq 0$ determines the stability of the model in both pre and post bounce scenarios. The square speed of sound diverges at the model's bouncing point within the context of Einstein's theory of gravity. This shows that the model could be unstable at the bouncing point and requires more investigation.

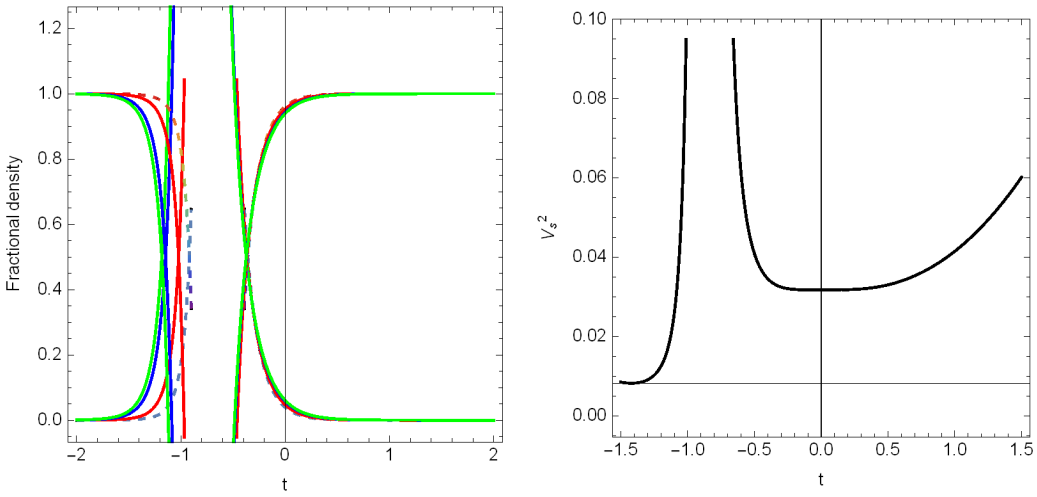

Figure 9. Evolution of fractional density (**left** panel) with $H_0 = (1.8, 1.7, 1.6, 1.5)$ and $B = 2.3$ for the lines coloured in Rainbow, Red, Blue, Green respectively and stability analysis (**right** panel) in the range of $H_0 < 2.5$ shown by Black line for bouncing model II.

3. Bounce Cosmology with Respect to E-Folding Number

For every bouncing layout associated with inflationary data, we have established the theory of perturbations for the framework of GCG evolution, and this is crucial to us. Particularly, the Hubble horizon contracts before the bounce phase and decays more quickly than the produced vacuum state fluctuations' wavelengths. After bouncing out of the Hubble radius, the fluctuations re-enter the inner regions of the horizon during the expanding phase. Now, we have thought about the e-folding time scale N [141,142], which is the base-e equivalent of doubling time in physics, is the period of time during which an exponentially expanding quantity rises by a factor of exp, related to the scale factor as given in spite of cosmic time t:

$$e^{-N} = \frac{a_0}{a} \ . \tag{34}$$

Alternatively, $N = ln(\frac{a}{a_0})$, which implies $H = \dot{N}$.

The e-folding number, $N = ln(\frac{a}{a_0})$, has been shown to be unaffected by perturbations in this measure; therefore, it may be used as a natural time coordinate instead of the cosmological time, t. Thus, we demonstrate that there is a straightforward relationship between the derivative of the fundamental equations with respect to the parameter N and the perturbation equations in the long wavelength limit. This finding suggests that the gauge used for the perturbation equations and the time coordinate used for the background equations are uniquely correlated.

Therefore, we have converted the cosmic time scale t into the e-folding time scale N and derived the thermodynamic pressure, density, EoS parameter, and an effective equation of state in terms of the e-fold number for both the models. Lastly, we have plotted pressure, density, and the effective equation of state against the time derivative of the e-fold number.

In Figures 10 and 11 we have plotted energy density, thermodynamic pressure, EoS parameter and effective EoS parameter with respect to cosmic time for bouncing model I and II respectively which are consistent with evolution of the universe.

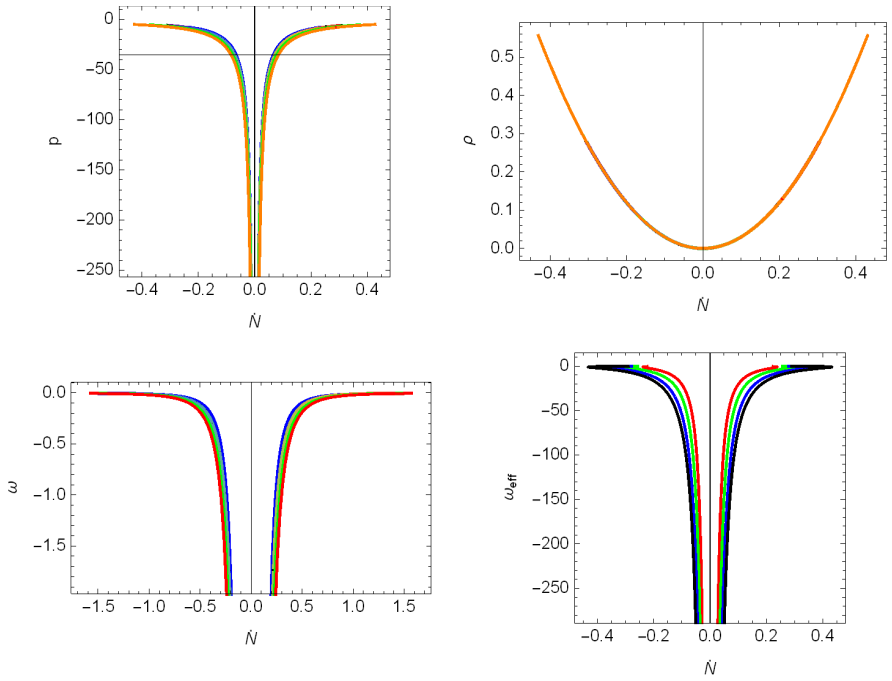

Figure 10. Symmetric behavior of thermodynamic pressure (**upper left** panel), density (**upper right** panel) with $\sigma = (0.34, 0.56, 0.86, 1.12)$, $\rho_{m0} = 0.32$, $a_0 = 10.6$, $\alpha = 0.6$ for the lines coloured in Orange, Red, Blue, Green respectively, and EoS parameter (**lower left** panel) and effective equation of state parameter (**lower right** panel) with previous all constraints for the lines coloured in Black, Red, Blue, Green respectively in terms of e-folding number for first bouncing model.

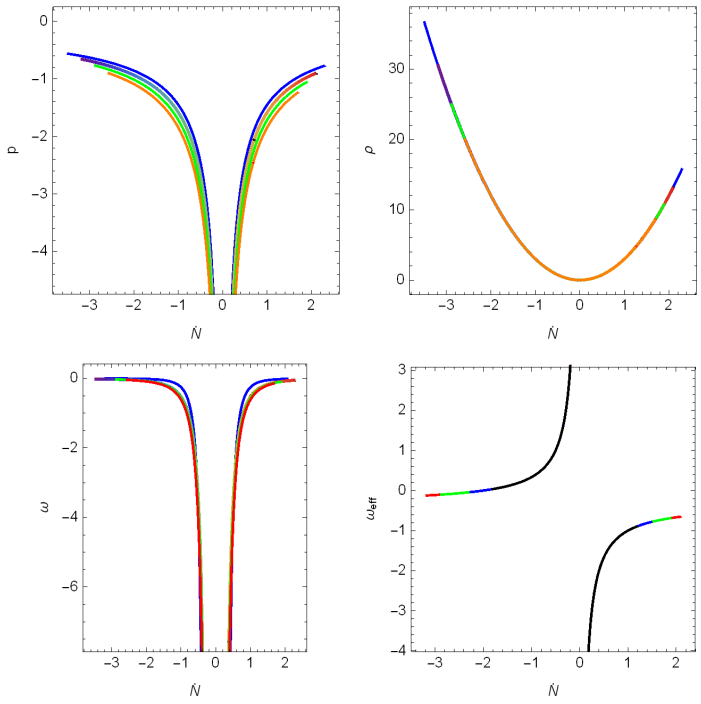

Figure 11. Symmetric behavior of thermodynamic pressure (**upper left** panel), density (**upper right** panel) with $H_0 = (1.8, 1.7, 1.6, 1.5)$, $\alpha = 0.6$ and $B = 2.3$ for the lines coloured in Orange, Red, Blue, Green respectively, EoS parameter (**lower left** panel) and effective equation of state parameter (**lower right** panel) with previous all constraints for the lines coloured in Black, Red, Blue, Green respectively in terms of e-folding number for second bouncing model.

4. Violation of Energy Conditions

In general relativity, high-energy physics, and cosmology, the null energy condition (NEC) [143–146] is traditionally assumed. This NEC criteria states that the energy density (ρ) and pressure (P) together remain non-negative for ideal fluids. The total energy density, or the Hubble parameter H, always falls in an expanding universe if the NEC is fulfilled. On the other hand, NEC fulfilment causes the total energy density to continuously rise in a shrinking universe, where $H < 0$. In this study we have investigated cosmological parameters of non-singular bouncing scenario. This kind of non-singular bounce uses a stress-energy that violates the NEC, hence whether it succeeds or fails depends on whether the NEC can be violated without causing pathologies. If we consider $\dot{H} = -\frac{1}{2}(\rho + p)$, we clearly understand that $\rho + p$ has to be necessarily negative in order for $\dot{H}$ to be positive. Thus, for a transition from pre-bounce contraction to post-bounce expansion, we require the violation of the null energy condition. It may be noted that the energy conditions (ECs) are a collection of linear equations that show that gravity is always attractive and that energy density cannot be negative. No linear combination of density and pressure, according to ECs, can be negative. They come from Raychaudhuri's equation and are needed in the investigation of wormholes and the thermodynamics of black holes. ECs are identified as

$$\frac{d\theta}{d\tau} = -\frac{1}{3}\theta^2 - \sigma_{\mu\nu}\sigma^{\mu\nu} + \omega_{\mu\nu}\omega^{\mu\nu} - R_{\mu\nu}u^\mu u^\nu \ , \tag{35}$$

$$\frac{d\theta}{d\tau} = -\frac{1}{2}\theta^2 - \sigma_{\mu\nu}\sigma^{\mu\nu} + \omega_{\mu\nu}\omega^{\mu\nu} - R_{\mu\nu}n^\mu n^\nu \ , \tag{36}$$

where the expansion factor is θ, the null vector is n^μ, and the shear term $\sigma^{\mu\nu}$ and the rotation term $\omega_{\mu\nu}$ are associated with the vector field u^μ . For attractive gravity, the constraints are

$$R_{\mu\nu}u^\mu u^\nu \geq 0 \tag{37}$$

$$R_{\mu\nu}n^\mu n^\nu \geq 0 \tag{38}$$

As a result, the energy conditions that may be obtained from a conventional GR under the assumption of a perfect fluid matter distribution are:

$$1.\ \ \rho + P \geq 0, \text{Null Energy Condition (NEC)}; \tag{39}$$

$$2.\ \ \rho + 3P \geq 0, and \quad \rho + P \geq 0, \text{Strong Energy Condition (SEC)}; \tag{40}$$

$$3.\ \ \rho > |P| \geq 0, \text{Dominant Energy Condition (DEC)}; \tag{41}$$

$$4.\ \ \rho \geq 0, and \quad \rho + P \geq 0, \text{Weak Energy Condition (WEC)}. \tag{42}$$

4.1. Energy Condition Investigation

In this section and next we have investigated energy conditions in the context of bounce and GCG scenario.

4.1.1. Bounce Model-I

We can obatin the energy density and thermodynamic pressure from Equations (15) and (16) as follows:

$$NEC = -12^{-\alpha}B\left(\frac{t^2\sigma^2}{(2+3t^2\sigma)^2}\right)^{-\alpha} + \frac{12t^2\sigma^2}{(2+3t^2\sigma)^2} \tag{43}$$

$$SEC = 3\left(-12^{-\alpha}B\left(\frac{t^2\sigma^2}{(2+3t^2\sigma)^2}\right)^{-\alpha} + \frac{4t^2\sigma^2}{(2+3t^2\sigma)^2}\right) \tag{44}$$

$$DEC = 12^{-\alpha}B\left(\frac{t^2\sigma^2}{(2+3t^2\sigma)^2}\right)^{-\alpha} + \frac{12t^2\sigma^2}{(2+3t^2\sigma)^2} \tag{45}$$

To achieve a successful non-singular bounce, the EoS parameter has to cross the phantom split and hence break the NEC. The following numbers show the breaches of energy criteria. The figures demonstrate that the bouncing epoch is not surrounded by a singularity. On the other hand, the energy conditions symmetrically evolve around the bouncing point. The energy conditions $\rho + P$ and $\rho + 3P$ deviate from their expected values in the vicinity of the bounce, as would be expected for a matter bounce scenario. This clear indication of an energy condition violation causes the model to evolve in the phantom phase.

4.1.2. Bounce Model-II

Here, we have obtained energy conditions from energy density and thermodynamic pressure of second bouncing model from Equations (26) and (27) as follows:

$$NEC = -48^{-\alpha}B\left(\frac{{H_0}^2(6+H_0t(6+H_0t(3+H_0t)))^2}{(24+H_0t(24+H_0t(12+H_0t(4+H_0t))))^2}\right)^{-\alpha} + \frac{48{H_0}^2(6+H_0t(6+H_0t(3+H_0t)))^2}{(24+H_0t(24+H_0t(12+H_0t(4+H_0t))))^2} \tag{46}$$

$$SEC = 3(-48^{-\alpha}B\left(\frac{{H_0}^2(6+H_0t(6+H_0t(3+H_0t)))^2}{(24+H_0t(24+H_0t(12+H_0t(4+H_0t))))^2}\right)^{-\alpha} + \frac{16{H_0}^2(6+H_0t(6+H_0t(3+H_0t)))^2}{(24+H_0t(24+H_0t(12+H_0t(4+H_0t))))^2}) \tag{47}$$

$$DEC = 48^{-\alpha}B\left(\frac{{H_0}^2(6+H_0t(6+H_0t(3+H_0t)))^2}{(24+H_0t(24+H_0t(12+H_0t(4+H_0t))))^2}\right)^{-\alpha} + \frac{48{H_0}^2(6+H_0t(6+H_0t(3+H_0t)))^2}{(24+H_0t(24+H_0t(12+H_0t(4+H_0t))))^2} \tag{48}$$

In Figure 12, we display the violation of the energy criterion for both models. The evolution of the energy conditions in *model I* is shown in the left panel, while the evolution of the energy conditions in *model II* is shown in the right panel. Additionally, we demonstrate in the figures that the strong energy condition (black line) is broken and the dominant energy condition (green line) is met for both the models. Near the bounce, the null energy condition (red line) is broken in first model and just barely broken in second model. Additionally, the violation of the strong energy condition when the null energy condition is broken is the evident phenomenon. The strong energy constraint, however, has been seen to be broken throughout the evolution of *model I* for the graphical representation, and, to a lesser extent, for *model II* around the bounce period. For both the models weak energy condition is also achieved (blue line) for pre and post bounce scenario. It is important to note that the non-singular bounce solution is related to the early universe's violation of the null energy requirement. The identical observation that supports the universe's bouncing solution has been made in the current work.

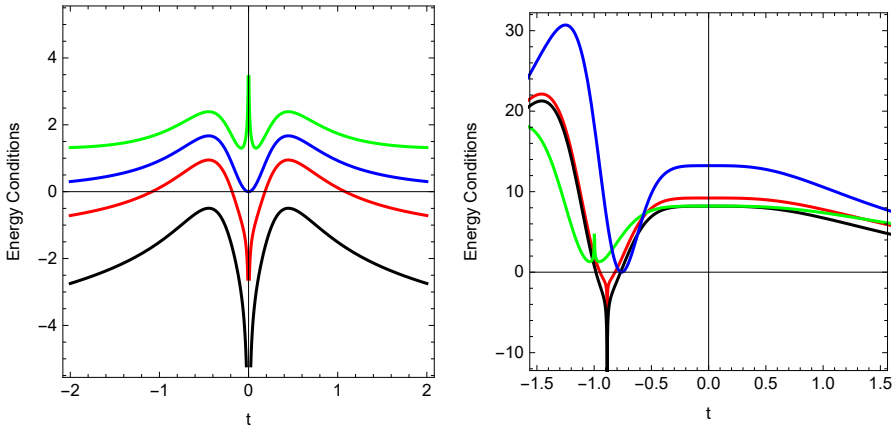

Figure 12. Behaviorof energy conditions for model I (**left** panel) and for model II (**right** panel) by the lines coloured in [(**NEC** by Red), (**SEC** by Black), (**DEC** by Green), (**WEC** by Blue)].

5. Roles of Geometrical Parameters

Geometrical parameters are crucial for analysing models in any gravity theory. In the section that follows, we employ a method known as "cosmography" [147–152] to describe the evolution of the universe. It is solely based on the cosmological principle and certain equivalence-principle-related conclusions. The words "cosmography" and "cosmokinematics" are interchangeable. Recall that kinematics is the branch of mechanics that explains body motion irrespective of the forces driving it. In this view, the kinematics of cosmic expansion are all that cosmography reflects. The laws of motion (Einstein's equation) plus some assumptions about the universe's substance make it possible to create the energy–momentum tensor, which is necessary to construct the fundamental cosmological variable $a(t)$. Cosmography is most effective when it can test any cosmological hypothesis that complies with the cosmological principle. Changes to general relativity or the addition of new elements (such as DM or DE) certainly alter the dependency $a(t)$, but they have no bearing whatsoever on the expansion of the universe's kinematics. The Hubble parameter $H(t)$, which measures the rate of the universe's expansion, is time-dependent. The deceleration parameter $q(t)$ is used to quantify this dependence. For $q < 0$, the scaling factor grows at an accelerated pace. When the deceleration parameter's sign was first specified, it appeared obvious that gravity was the primary factor controlling the dynamics of the universe and that this should cause the universe to expand more slowly. The natural desire to deal with positive amounts thus dictated the sign's selection. This decision proved to be incongruent with the dynamics that could be seen and turned into a historical puzzle. It is helpful to think about the expanded set of the parameters in order to understand the kinematics of the cosmic expansion in greater detail.

$$H(t) = \frac{1}{a}\frac{da}{dt}(HubbleParameter) \tag{49}$$

$$q(t) = -\frac{1}{a}\frac{d^2a}{dt^2}(H(t))^{-2}, \text{Deceleration Parameter} \tag{50}$$

$$j(t) = -\frac{1}{a}\frac{d^3a}{dt^3}(H(t))^{-3}, \text{Jerk Parameter} \tag{51}$$

$$s(t) = -\frac{1}{a}\frac{d^4a}{dt^4}(H(t))^{-4}, \text{Snap Parameter} \tag{52}$$

$$s(t) = -\frac{1}{a}\frac{d^5a}{dt^5}(H(t))^{-5}, \text{Lerk Parameter} \tag{53}$$

Other geometrical characteristics, such as the jerk parameter (j) and snap parameter (s), are included in addition to the Hubble and deceleration parameters. The snap parameter

monitors the jerk rate, whereas the jerk parameter determines the rate of acceleration change. The sign of j is crucial to determining whether the universe evolves since the deceleration parameter is insufficient to explain all of cosmic dynamics. It is important to be aware that a positive jerk parameter denotes a shift in the universe's expansion at some time in its history. The state finder pair, also known as the (j,s) pair, may be used to differentiate between various dark energy theories.

5.1. Bounce Model I

In this subsection we have derived cosmographic parameters for first bouncing model.

$$q(t) = \frac{1}{2} - \frac{1}{t^2\sigma} \tag{54}$$

$$j(t) = 1 - \frac{6}{t^2\sigma} \tag{55}$$

$$s(t) = -\frac{7}{2} + \frac{6\left(-1 + 7t^2\sigma\right)}{t^4\sigma^2} \tag{56}$$

Figure 13 displays the cosmographic parameters' graphical behaviour. Regardless of the typical values of σ, all of these parameters suffer singularity during the bounce epoch and are symmetric around the bounce point. The deceleration parameter's positive value suggests a decelerating universe, whereas its negative value indicates an accelerating universe. The deceleration parameter, which approaches -1 at early and late times, validates the accelerating behaviour of the mathematical models and is in line with the current observational value of q. In the figures of the right panel, we have highlighted the geometrical parameters' late-time behaviour. In accordance with the late-time graphical behaviour that agrees with the most recent observational estimate of the deceleration parameter at the current age of the Universe. It completely stays in the negative range, initially decreasing and then increasing after encountering a singularity at the bounce, finally settling at -1. The jerk parameter demonstrates unfavourable behaviour throughout and changes from a huge value to a sharp fall to a singularity to a sharp increase once more. As we move away from the bounce epoch, the snap parameter crosses zero again before reaching its maximum value. At the same time, the snap parameter displays single behaviour in the negative profile.

5.2. Bounce Model II

Cosmographic parameters for second bouncing model as follows:

$$q(t) = -\frac{3(2 + H_0t(2 + H_0t))(24 + H_0t(24 + H_0t(12 + H_0t(4 + H_0t))))}{4(6 + H_0t(6 + H_0t(3 + H0t)))^2} \tag{57}$$

$$j(t) = \frac{3(1 + H_0t)(24 + H_0t(24 + H_0t(12 + H_0t(4 + H_0t))))^2}{8(6 + H_0t(6 + H_0t(3 + H_0t)))^3} \tag{58}$$

$$s(t) = \frac{3(24 + H_0t(24 + H_0t(12 + H_0t(4 + H_0t))))^3}{32(6 + H_0t(6 + H_0t(3 + H_0t)))^4} \tag{59}$$

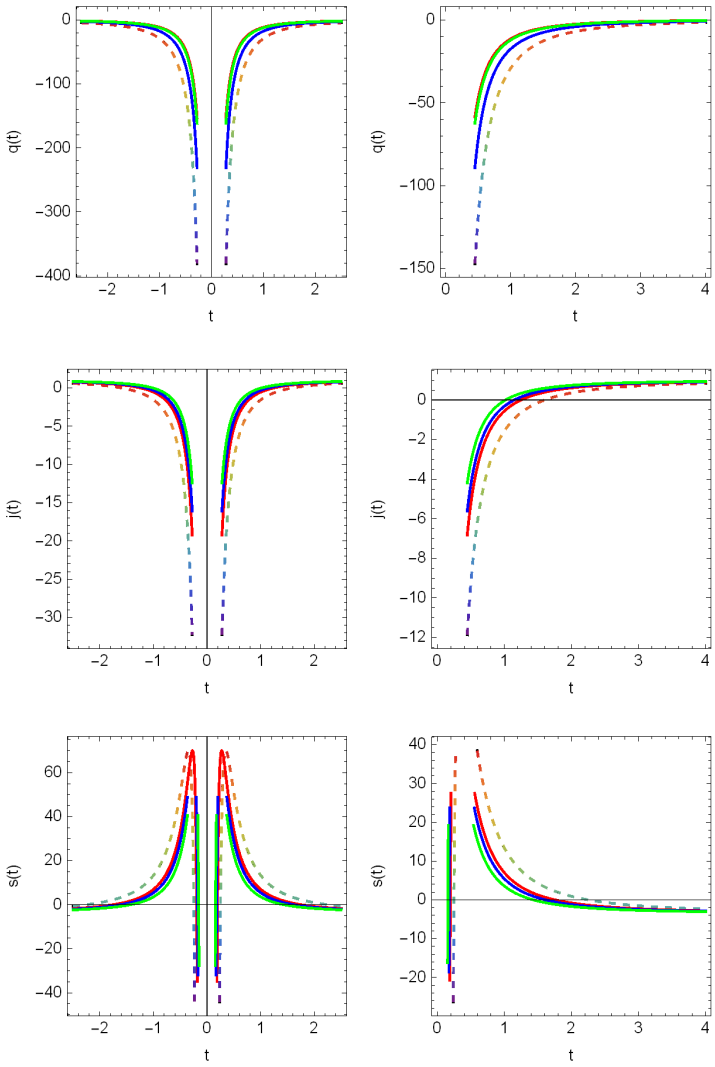

Figure 13. Behavior of geometrical parameters for model I with $\sigma = (0.34, 0.56, 0.86, 1.12)$, $\rho_{m0} = 0.32$, $a_0 = 10.6$, $\alpha = 0.6$ for the lines coloured in Rainbow, Red, Blue, Green respectively.

The graphical behaviour of the cosmographic parameters is shown in Figure 14. All of these parameters experience singularity during the bounce period and are symmetric around the bounce point, regardless of the typical values of H_0. A universe that is decelerating is suggested by a positive value for the deceleration parameter, whereas an accelerating world is suggested by a negative value. The cosmos is accelerating, as evidenced by the growth of the deceleration parameter towards a negative value, or $q \to -0.8$, post bouncing point. Deceleration parameter is through out negative in the history of the evolution for this case. Similarly, the toy universe model's growth rate is determined by jerk (j) and snap (s).

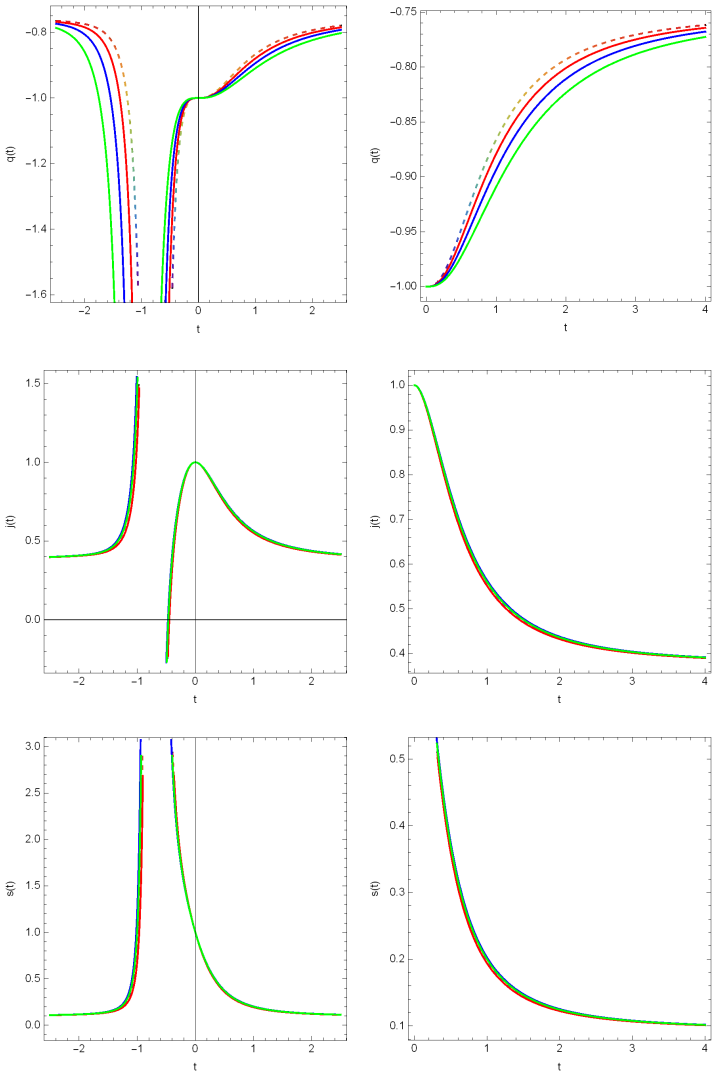

Figure 14. Behavior of geometrical parameters for model II with $H_0 = (1.8, 1.7, 1.6, 1.5)$ for the lines coloured in Rainbow, Red, Blue, Green respectively .

6. Hubble Flow Dynamics

In the early universe, cosmic inflation is one of the main paradigms to explain the cosmological parameters, which contain phases of exponential expansion of the universe, and it fulfills the conditions to initiate inhomogeneities on cosmological scales. We consider the Hubble flow parameters [153–158], defined by

$$\epsilon_{i+1} = \frac{dln\epsilon_i}{dN}. \tag{60}$$

where N is the e-folding time scale.

$$\epsilon_1 = 1 - \frac{\ddot{a}}{aH^2} = -\frac{\dot{H}}{H^2}. \tag{61}$$

$$\epsilon_2 = \frac{\dot{\epsilon_1}}{H\epsilon_1}. \tag{62}$$

For inflation, $\ddot{a} > 0$, ϵ_1 has to be less than 1. Additionally, it is very obvious for a vanishing inflationary epoch ϵ_1 that it has to take the value of unity.

Here, Figure 15 upper panel and lower panel both show the parameters of the Hubble flow, respectively for both the models. In first model, ϵ_1 and ϵ_2 is symmetrical about the turnaround point, as seen in Figure 15 upper panel. ϵ_1 displays a decreasing symmetrical pattern in both the pre and post-bounce scenarios. As a result, we comprehend that across

the bounce, $\epsilon_1 << 1$, meets the prerequisite for inflation. But in the first model, we could not see the exit of inflation as $\epsilon_2 >> 0$, which needs further investigation. In Figure 15 lower panel ϵ_1 shows a decreasing pattern in pre-bounce scenario and increasing pattern in post-bounce scenario. But in pre and post both the cases $\epsilon_1 << 1$, meets the prerequisite for inflation. In the case of the pre-bounce, $H < 0$, ϵ_1 and $\dot{\epsilon_1} < 0$. In Figure 15 lower panel, we can see that right before the bounce, $\epsilon_2 < 0$, which supports the theory, and immediately after the bounce, $H > 0$ and $epsilon_2$, which also supports inflation, is less than zero. At that point, ϵ_2 turns positive. In this case also we could not see the exit of inflation as ϵ_1 is not crossing 1.

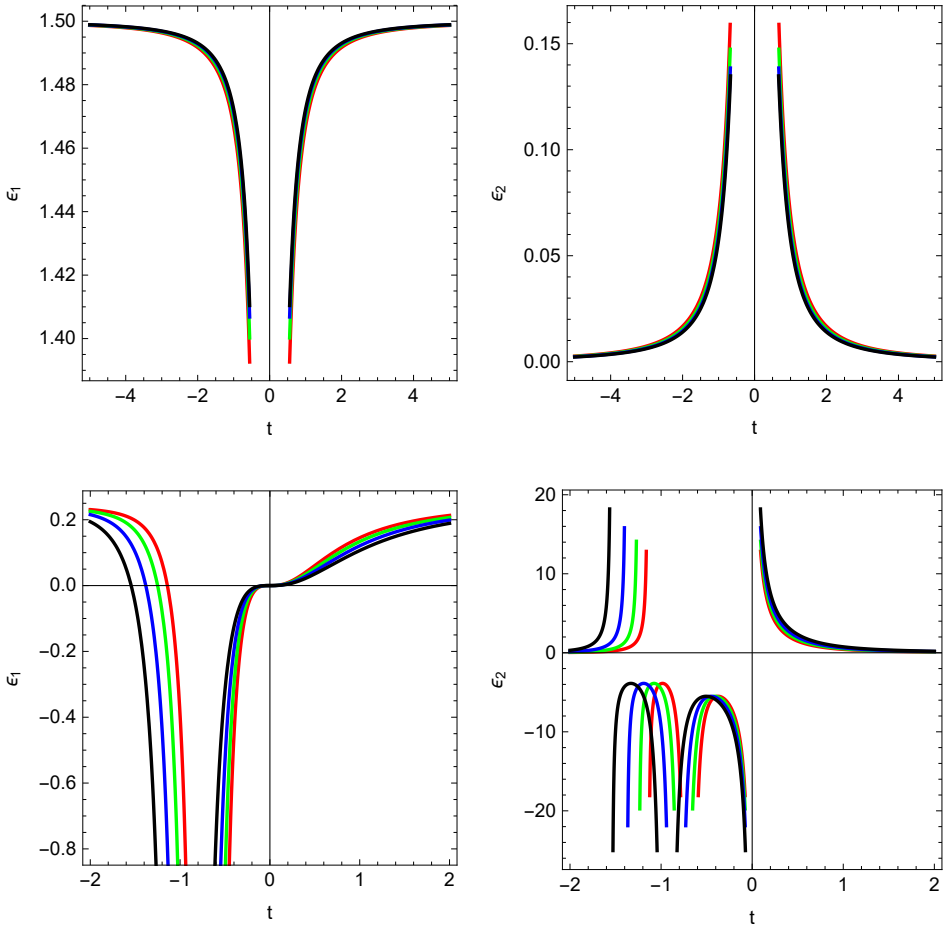

Figure 15. Behavior of Hubble flow parameters for model I (**upper** panel) with $\sigma = (0.34, 0.56, 0.86, 1.12)$, $\rho_{m0} = 0.32$, $a_0 = 10.6$, $\alpha = 0.6$ for the lines coloured in Red, Blue, Green, Black respectively and for model II (**lower** panel) with $H_0 = (1.8, 1.7, 1.6, 1.5)$ for the lines coloured in Red, Blue, Green, Black respectively.

7. Inflation via Scalar Field

The study of the dynamical aspects of scalar fields in cosmology is motivated by the prediction of the presence of scalar fields in a number of fundamental physics [159–165]. In fact, the study of the early cosmos, particularly the study of inflation, is greatly aided by scalar field cosmological models [166]. The late-time evolution of scalar field models has also been receiving a lot of attention recently. The so-called "quintessential" scalar field models (or slowly decaying cosmological constant models) produce a residual scalar field that adds to the universe's current energy density. This residual scalar field may help solve the dark matter issue and predict an effective cosmological constant, aligning with observations of the universe's accelerated expansion [167,168].

Inflation [169–171] is an excellent paradigm that not only corrects the aforementioned issues but also gives us a quantum mechanical mechanism for the formation of primor-

dial gravity waves, scalar (density) perturbations, and tensor perturbations. The density perturbations that inflation predicts would have a virtually flat spectrum must have their amplitudes fixed via COBE normalization. In this section, we consider the scalar field ϕ, which depends on a potential $V(\phi)$ and is minimally coupled. Therefore, in a curved space–time, the Lagrangian will be

$$\mathcal{L}_\phi = -\frac{1}{2}\mathcal{G}^{\alpha\beta}\partial_\alpha\phi\partial_\beta\phi - V(\phi) \ . \tag{63}$$

Here, $\mathcal{G}^{\alpha\beta}$ is the metric tensor and $\partial_\alpha\phi$ and $\partial_\beta\phi$ are covariant derivatives. Here, we have considered the scalar field ϕ and the effective GCG energy density $\tilde{\rho_c}$; thus, the isotropic pressure incorporated with bulk viscosity will be

$$\tilde{\rho_c} = \frac{\dot{\phi}^2}{2} + V(\phi) \ . \tag{64}$$

$$\tilde{p_c} = \frac{\dot{\phi}^2}{2} - V(\phi) \ . \tag{65}$$

We now wish to use a scalar field to illustrate inflationary dynamics. In the context of a scalar field framework, we have examined a flat FRW universe that is filled with viscous GCG.

7.1. Bounce Model I

Here, we obtain the total energy density from Equations (15) and (16). By using Equations (15) and (16) in Equations (49) and (50), we obtain the expression of $\dot{\phi}^2$ and $V(\phi)$ as a function of t, as follows:

$$\dot{\phi}^2 = -12^{-\alpha}B\left(\frac{t^2\sigma^2}{(2+3t^2\sigma)^2}\right)^{-\alpha} + \frac{12t^2\sigma^2}{(2+3t^2\sigma)^2} \tag{66}$$

$$V(\phi(t)) = \frac{1}{2}\left(12^{-\alpha}B\left(\frac{t^2\sigma^2}{(2+3t^2\sigma)^2}\right)^{-\alpha} + \frac{12t^2\sigma^2}{(2+3t^2\sigma)^2}\right) \tag{67}$$

We have plotted $(V(\phi) - \dot{\phi}^2)$ and $\dot{\phi}^2$ with respect to cosmic time in the following figure.

7.2. Bounce Model-II

By using Equations (26) and (27) in Equations (64) and (65), we obtain $V(\phi)$ and $\dot{\phi}^2$ as follows:

$$V(\phi(t)) = \frac{1}{2}\left(48^{-\alpha}B\left(\frac{{H_0}^2(6+H_0t(6+H_0t(3+H_0t)))^2}{(24+H_0t(24+H_0t(12+H_0t(4+H_0t))))^2}\right)^{-\alpha} + \frac{48H_0^2(6+H_0t(6+H_0t(3+H_0t)))^2}{(24+H_0t(24+H_0t(12+H_0t(4+H_0t))))^2}\right) \tag{68}$$

$$\dot{\phi}^2 = -48^{-\alpha}B\left(\frac{H_0^2(6+H_0t(6+H_0t(3+H_0t)))^2}{(24+H_0t(24+H_0t(12+H_0t(4+H_0t))))^2}\right)^{-\alpha} + \frac{48H_0^2(6+H_0t(6+H_0t(3+H_0t)))^2}{(24+H_0t(24+H_0t(12+H_0t(4+H_0t))))^2} \tag{69}$$

Evolution of the scalar field is represented in Figure 16 for model I and in Figure 17 for model II. In Figure 16 (left panel) we can demonstrate that the scalar field exhibits a decreasing pattern before and after to the bounce and that it takes an endless amount of time to reach the turn-around point. In Figure 16 (right panel) we have plotted $\dot{\phi}^2$ which is symmetric around the bouncing point. The scalar field starts to exhibit increasing behaviour close to the bounce event in Figure 17 (left panel). In Figure 17 (left panel), the difference $(V(\phi) - \dot{\phi}^2)$ is displayed. It reveals that after the bounce, $(V(\phi) > \dot{\phi}^2)$, which is compatible

with the inflationary universe after the bounce as observed in the preceding paragraph as $\dot{\phi}^2$) is negative in post-bounce scenario, shown in Figure 17 (right panel).

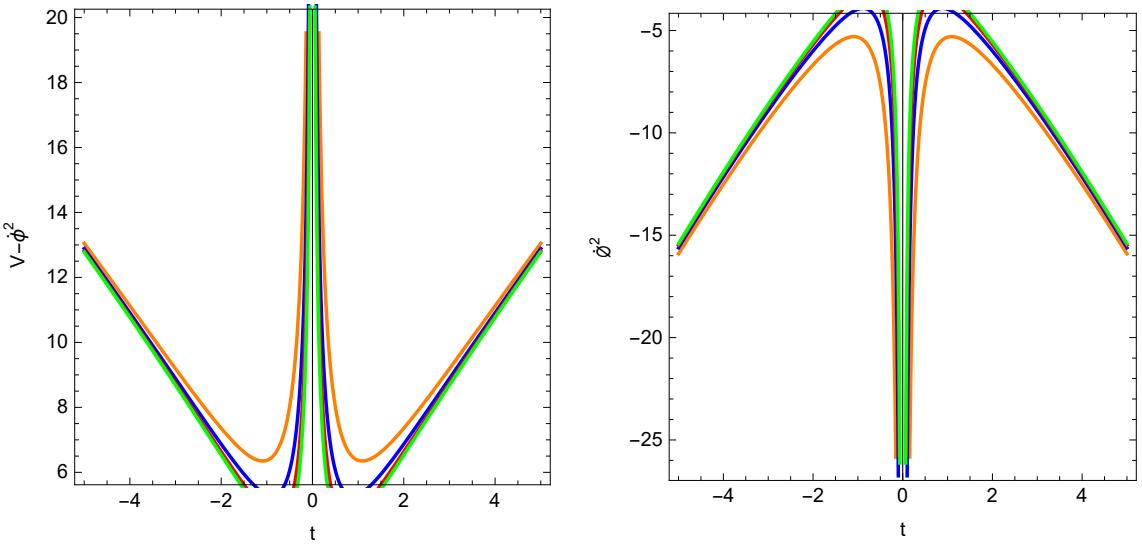

Figure 16. Evolution of the scalar field $(V(\phi) - \dot{\phi}^2)$(**left** panel) and $\dot{\phi}^2$(**right** panel) for model I with $\sigma = (0.34, 0.56, 0.86, 1.12)$, $\rho_{m0} = 0.32$, $a_0 = 10.6$, $\alpha = 0.6$ for the lines coloured in Red, Blue, Green, Orange respectively.

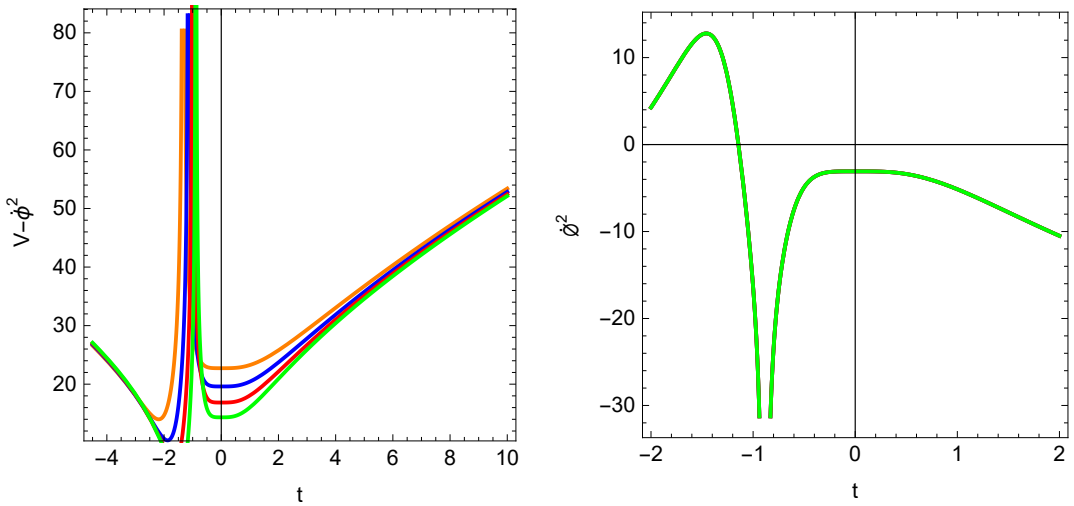

Figure 17. Evolution of the scalar field $(V(\phi) - \dot{\phi}^2)$(**left** panel) with $H_0 = (1.8, 1.7, 1.6, 1.5)$ and $B = 2.5$ for the lines coloured in Red, Blue, Green, Orange respectively and $\dot{\phi}^2$ (**right** panel) in the range of $H_0 < 2.5$ shown by overlapping Green line for model II.

8. Concluding Remarks and Future Developments

First, we took into consideration the [136,137] bouncing scale factors from the literature. The authors of the work cited in reference [136] examined the possibility of using $f(T)$ gravity to implement the matter bounce cosmology. The authors of [137] extracted the de Sitter scale factor solution, $a(t) = a_0 e^{H_0 t}$, using a_0 and H_0 as integration constants. In this paper, we looked more closely at a modified scale factor to produce the bounce. The cosmic scale factor, which connects distances at different points in time, is a time-dependent function that depicts the universe's expansion. The Hubble parameter extends from the early universe and vanishes at the epoch $t = 0$ before continuing to climb, as expected given the bouncing behavior (Figure 1 (left panel)). Although the bounce singularity is visible in Figure 1 (right panel), there is also a nonsingular bounce in the middle panel. First, using the bouncing scale factors from Equation (2) and their modified versions

from Equation (6) along with a background fluid composed of generalized Chaplygin Gas (GCG), we compared the nonsingular bounce cosmology. Last but not least, we showed a singular bounce using the updated scale factor from Equation (8). The GCG energy density decreases due to contraction in the pre-bounce scenario, reaches its lowest point at $t = 0$ during the bounce, and rises due to expansion following the bounce. According to the inflationary theory of the universe, this graphic shows a rapid increase in density brought on by inflation, followed by a stable increase in density over the following epochs of the cosmos.

By avoiding an initial singularity [159], bouncing cosmologies offer an alternative to typical expanding cosmologies. The cost is caused by speculating on some potential new physics at the bounce, which leads to the universe expanding again after a brief period of contraction. It is still uncertain if isotropization may actually occur in physically driven circumstances because viscosity is frequently simply parametrized in this setting. Although the introduction of viscosity coefficients in cosmology has a long history, their physical significance has typically been thought to be marginal or at the very least subdominant. According to theories about the very early universe, neutrino decoupling is when viscosity is thought to have the greatest influence. The authors presented microphysical manifestations of viscosity and the effects of anisotropies in the early universe [105]. In our current study, the energy density is continuously and carefully developing in the background. The bounce is clearly observable at $t = 0$. The dark energy era and GCG as background fluid are supported by thermodynamic pressure, which is a negative pressure. In Figure 3, we displayed the bulk viscous pressure and viscosity coefficient. According to Figure 3, the viscosity coefficient is positive and the bulk viscous pressure is negative in the early universe. As a result, even at an early stage, the bulk viscosity has a considerable impact. The point where the matter is bouncing is where Π and ξ diverge. Once more, it is clear that the denominator of this equation, Equation (15), reaches a value of zero at the point of bouncing, $t = 0$. The growth of the reconstructed EoS parameter diverges as a result, as seen in Figure 4 (left panel). Furthermore, in pre- and post-bounce circumstances, the EoS parameter crosses a phantom border. However, the right panel's effective EoS parameter avoids the Big Rip singularity in the post-bounce scenario but exhibits phantom-like behavior close to the bouncing point.

We have also talked about the fractional energy density for the two examples being investigated. The depiction of the reconstructed fractional densities across cosmic time t in Figure 5 (left panel) makes it clear that the universe is transitioning from a structure where matter dominates to a structure where energy dominates. As previously indicated, the picture demonstrates how the GCG background evolution fluid suggests that dark matter is weakening over time. We can see changes as a matter-dominated structure gives way to an energy-dominated structure. As previously indicated, the figure demonstrates how dark matter is becoming weaker over time while dark energy is becoming stronger with the aid of the GCG background evolution fluid. The squared speed of sound diverges at the model's bouncing point in the context of Einstein's theory of gravity. This raises the possibility that the model is unstable at the bouncing point and necessitates additional study. In the context of Einstein's theory of gravity, we have performed a stability analysis using the squared speed of sound Equation (25). The value of $V_s ge 0$ determines the model's stability. A negative number suggests that the model is unstable. We have plotted V_s^2 with cosmic time t and added the squared speed of sound below for GCG reconstruction approaches in Einstein's framework for the bouncing scale factor from Equation (6).

The EoS parameter must cross the phantom split and break the NEC to achieve a successful nonsingular bounce. The following numbers show the breaches of energy criteria. The figures demonstrate that a singularity does not surround the bouncing epoch. On the other hand, the energy conditions symmetrically evolve around the bouncing point. The energy conditions $\rho + P$ and $\rho + 3P$ deviate from their expected values near the bounce, as would be expected for a matter-bounce scenario. This clear indication of an energy condition violation causes the model to evolve in the phantom phase. In Figure 11, we

display the violation of the energy criterion for both models. The evolution of the energy conditions in *modelI* is shown in the left panel, while the evolution in *modelII* is shown in the right panel. Additionally, we demonstrate in the figures that the strong energy condition (black line) is broken and the dominant energy condition (green line) is met. The null energy condition (red line) is barely broken near the bounce. Additionally, violating the strong energy condition when the null energy condition is broken is an evident phenomenon. The strong energy constraint, however, has been seen to be broken throughout the evolution of *modelI* for the graphical representation and, to a lesser extent, for *modelII* around the bounce period. It is important to note that the nonsingular bounce solution is related to the early universe's violation of the null energy requirement. An identical observation that supports the universe's bouncing solution has been made in the current work. To further consolidate our understanding, we have incorporated a cosmographic analysis for both the cases in Figures 13 and 14. The jerk parameter (j) and snap parameter (s) are included with the Hubble and deceleration parameters. The snap parameter monitors the jerk rate, whereas the jerk parameter determines the rate of change in the acceleration. The sign of j is crucial to determining whether the universe evolves since the deceleration parameter cannot explain all cosmic dynamics. Of note, a positive jerk parameter denotes a shift in the universe's expansion at some time in its history. The state finder pair, also known as the (j,s) pair, may be used to differentiate between various dark energy theories. In our study, a shift of sign from negative to positive in the case of the jerk parameter in a post-bounce scenario is realized in both cases. The bahaviour is consistent with pre-bounce contraction and evident from the transition from negative to positive. One important outcome is that the realization of the ΛCDM fixed point is impossible for the truncated scale factor. In contrast, for the first case, the statefinder trajectory realizes the ΛCDM fixed point in the expansion phase of the universe.

As we studied the Hubble flow dynamics, we observed in Figure 15 that the Hubble flow parameter ϵ_1 is <1 in the case of the truncated scale factor. Hence, the inflationary cosmology is realizable in this case. On the contrary, this is not the case for the first choice of scale factor. Thus, we can interpret that the second choice of the scale factor can realize pre-bounce contraction and post-bounce inflationary expansion. In conclusion, let us comment on the outcomes of the current study with respect to some existing works. A recent study [154] demonstrated a model of a superbounce scenario and showed that if the ekpyrotic phase persisted until the Big Crunch, the model bounced at the relevant epoch. As a future study, we propose to look at the bounce cosmology in modified gravity theories, such as $f(T)$, and to study the consequences in a superbounce situation for various equations of state. A stable inflationary hypothesis proposed in [164], based on the anomaly-induced action of gravity, predicted an exceedingly rapid exponential expansion of the universe. In [159], it was shown that it is possible to obtain one pre-inflationary semiclassical cosmological solution that is consistent with stable exponential growth. In view of this, we intend to extend our future study towards obtaining a pre-inflationary semiclassical cosmological solution that is consistent with the stable exponential growth with the scale factors under consideration [165].

In conclusion, let us comment on the newness of the outcomes of the current study with respect to the past works on bounce cosmology in dark energy models including modified gravity theories. One remarkable work in this direction is by [97], where the authors concentrated on modified gravity aspects of early late-time acceleration, and bounce dynamics and methodically outlined how a coherent account of inflation with the dark energy era may be provided by utilizing the modified gravity framework through a unified description of inflation with dark energy era. In line with the critical review presented in [161], the current study presents bounce dynamics with Chaplygin gas as the fluid, whose equation of state depicts the history of a universe moving through an intermediary period from a phase where non-relativistic matter predominates to a phase where a cosmological constant predominates. Another noteworthy work in this direction is [97], where the authors showed that $F(R)$ gravity can describe a type IV singular bouncing cosmological

evolution. In this context, we would like to mention that the current study has considered the incorporation of the bulk viscosity into the bounce cosmology, and a viscous version of Chaplygin gas has been investigated for bounce realization. Following [97], we propose to extend this work in an $F(R)$ framework as a future study. At this juncture, we would also like to mention that [105] developed an energy conservation equation from a holographic perspective while studying bounce cosmology using a generalized Nojiri–Odintsov holographic cut-off [167]. Additionally, these authors showed how the holographic bounce and viscous fluid bounce are related. Contrary to the previous study, the current work explored the cosmology of viscous bounces and also demonstrated a cosmographic analysis and inflation via a scalar field in the Chaplygin gas model.

Author Contributions: All authors made equal contributions to the work reported in this paper. All authors read and agreed to the published version of the manuscript.

Funding: This research was funded by Council of Scientific and Industrial Research OF FUNDER grant number 03(1420)/18/EMR-II.

Data Availability Statement: Not applicable.

Acknowledgments: The authors sincerely acknowledge the constructive suggestions by the anonymous reviewers. Surajit Chattopadhyay acknowledges financial support from the Council of Scientific and Industrial Research (Government of India) with Grant No. 03(1420)/18/EMR-II.

Conflicts of Interest: The authors declare no conflict of interest.

References

1. Odintsov, S.D.; Oikonomou, V.K. Big bounce with finite-time singularity: The F(R) gravity description. *Int. J. Mod. Phys.* **2017**, *26*, 1750085. [CrossRef]
2. Odintsov, S.D.; Oikonomou, V.K. ΛCDM bounce cosmology without ΛCDM: The case of modified gravity. *Phys. Rev.* **2015**, *91*, 064036.
3. Nojiri, S.I.; Odintsov, S.D.; Saridakis, E.N. Holographic bounce. *Nucl. Phys.* **2019**, *949*, 114790. [CrossRef]
4. Salehi, A. Bouncing universe in the presence of an extended Chaplygin gas. *Phys. Rev. D.* **2016**, *94*, 123519. [CrossRef]
5. Perlmutter, S.; Aldering, G.; Deustua, S.; Fabbro, S.; Goldhaber, G.; Groom, D.E.; Kim, A.G.; Kim, M.Y.; Knop, R.A.; Nugent, P.; et al. Cosmology from type Ia supernovae. *arXiv* **1998**, arXiv:astro-ph/9812473.
6. Enqvist, K.; Sloth, M.S. Adiabatic CMB perturbations in pre-Big-Bang. *Nucl. Phys.* **2002**, *626*, 395–409. [CrossRef]
7. Spergel, D.N.; Bean, R.; Doré, O.; Nolta, M.R.; Bennett, C.L.; Dunkley, J.; Hinshaw, G.; Jarosik, N.E.; Komatsu, E.; Page, L.; et al. Three-year Wilkinson Microwave Anisotropy Probe (WMAP) observations: Implications for cosmology. *Astrophys. J. Suppl. Ser.* **2007**, *170*, 377. [CrossRef]
8. Macciò, A.V.; Dutton, A.A.; Van Den Bosch, F.C. Concentration, spin and shape of dark matter haloes as a function of the cosmological model: WMAP 1, WMAP 3 and WMAP 5 results. *Mon. Not. R. Astron. Soc.* **2008**, *391*, 1940–1954.
9. Tegmark, M.; Strauss, M.A.; Blanton, M.R.; Abazajian, K.; Dodelson, S.; Sandvik, H.; Wang, X.; Weinberg, D.H.; Zehavi, I.; Bahcall, N.A.; et al. Cosmological parameters from SDSS and WMAP. *Phys. Rev.* **2004**, *69*, 103501.
10. Eskilt, J.R.; Komatsu, E. Improved constraints on cosmic birefringence from the WMAP and Planck cosmic microwave background polarization data. *Phys. Rev.* **2022**, *106*, 063503.
11. Hinshaw, G.; Larson, D.; Komatsu, E.; Spergel, D.N.; Bennett, C.; Dunkley, J.; Nolta, M.R.; Halpern, M.; Hill, R.S.; Odegard, N.; et al. Nine-year Wilkinson Microwave Anisotropy Probe (WMAP) observations: Cosmological parameter results. *Astrophys. J. Suppl. Ser.* **2013**, *208*, 19.
12. Chen, S.F.; Lee, H.; Dvorkin, C. Precise and accurate cosmology with CMB× LSS power spectra and bispectra. *J. Cosmol. Astropart. Phys.* **2021**, *2021*, 30.
13. Holman, R.; Mersini-Houghton, L.; Takahashi, T. Cosmological avatars of the landscape. II. CMB and LSS signatures. *Phys. Rev.* **2008**, *77*, 063511. [CrossRef]
14. Pacaud, F.; Pierre, M.; Adami, C.; Altieri, B.; Andreon, S.; Chiappetti, L.; Detal, A.; Duc, P.A.; Galaz, G.; Gueguen, A.; et al. The XMM-LSS survey: The Class 1 cluster sample over the initial 5 deg2 and its cosmological modelling. *Mon. Not. R. Astron. Soc.* **2007**, *382*, 1289–1308. [CrossRef]
15. Garriga, J.; Pogosian, L.; Vachaspati, T. Forecasting cosmic doomsday from CMB-LSS cross-correlations. *Phys. Rev.* **2004**, *69*, 063511.
16. Anand, S.; Chaubal, P.; Mazumdar, A.; Mohanty, S. Cosmic viscosity as a remedy for tension between PLANCK and LSS data. *J. Cosmol. Astropart. Phys.* **2017**, *2017*, 5. [CrossRef]
17. Iguchi, H.; Nakamura, T.; Nakao, K.I. Is dark energy the only solution to the apparent acceleration of the present universe? *Prog. Theor. Phys.* **2002**, *108*, 809–818.

18. Turner, M.S. The dark side of the universe: From Zwicky to accelerated expansion. *Phys. Rep.* **2000**, *333*, 619–635. [CrossRef]
19. Copel, E.J.; Sami, M.; Tsujikawa, S. Dynamics of dark energy. *Int. J. Mod. Phys.* **2006**, *15*, 1753–1935.
20. Dirac, P.A.M. *General Theory of Relativity (Vol. 50)*; Princeton University Press: Princeton, NJ, USA, 1996.
21. Anderson, J.L. *General Relativity: Gravitation and Cosmology. Principles and Applications of the General Theory of Relativity*; Weinberg, S., Ed.; Wiley: New York, NY, USA, 1973; pp. 1227–1228.
22. Mukhanov, V.F.; Feldman, H.A.; Brandenberger, R.H.; Theory of cosmological perturbations. *Phys. Rep.* **1992**, *215*, 203–333. [CrossRef]
23. Gómez-Valent, A.; Sola, J.; Basilakos, S.; Dynamical vacuum energy in the expanding Universe confronted with observations: A dedicated study. *J. Cosmol. Astropart. Phys.* **2015**, *01*, 004. [CrossRef]
24. Carroll, S.M. The cosmological constant. *Living Rev. Relativ.* **2001**, *4*,1–56. [PubMed]
25. Cohen, A.G.; Kaplan, D.B.; Nelson, A.E. Effective field theory, black holes, and the cosmological constant. *Phys. Rev. Lett.* **1999**, *82*, 4971. [CrossRef]
26. Hsu, S.D. Entropy bounds and dark energy. *Phys. Lett. B* **2004**, *594*,13–16. [CrossRef]
27. Piran, T. Gamma-Ray Bursts-a Primer For Relativists. In *General Relativity and Gravitation*; World Scientific: Singapore, 2002; pp. 259–275.
28. Weinberg, S. The cosmological constant problem. *Rev. Mod. Phys.* **1989**, *61*, 1. [CrossRef]
29. Zel'Dovich, Y.B. The cosmological constant and the theory of elementary particles. *Sov. Phys. Uspekhi* **1968**, *11*, 381. [CrossRef]
30. Sahni, V. The cosmological constant problem and quintessence. *Class. Quantum Gravity* **2002**, *19*, 3435. [CrossRef]
31. Padmanabhan, T. Cosmological constant—The weight of the vacuum. *Phys. Rep.* **2003**, *380*, 235–320. [CrossRef]
32. Wu, J.P.; Ma, D.Z.; Ling, Y. Quintessence reconstruction of the new agegraphic dark energy model. *Phys. Lett.* **2008**, *663*, 152–159. [CrossRef]
33. Dutta, S.; Saridakis, E.N.; Scherrer, R.J. Dark energy from a quintessence (phantom) field rolling near a potential minimum (maximum). *Phys. Rev.* **2009**, *79*, 103005. [CrossRef]
34. Zhang, J.; Zhang, X.; Liu, H. Agegraphic dark energy as a quintessence. *Eur. Phys. J. C* **2008**, *54*, 303–309.
35. Singh, P.; Sami, M.; Dadhich, N. Cosmological dynamics of a phantom field. *Phys. Rev.* **2003**, *68*, 23522.
36. Nojiri, S.I.; Odintsov, S.D.; Tsujikawa, S. Properties of singularities in the (phantom) dark energy universe. *Phys. Rev.* **2005**, *71*, 063004. [CrossRef]
37. Chattopadhyay, S.; Debnath, U. Interaction between phantom field and modified Chaplygin gas. *Astrophys. Space Sci.* **2010**, *326*, 155–158.
38. Nojiri, S.I.; Odintsov, S.D. Quantum de Sitter cosmology and phantom matter. *Phys. Lett.* **2003**, *562*, 147–152. [CrossRef]
39. Nojiri, S.I.; Odintsov, S.D. Inhomogeneous equation of state of the universe: Phantom era, future singularity, and crossing the phantom barrier. *Phys. Rev.* **2005**, *72*, 23003. [CrossRef]
40. Cai, Y.F.; Saridakis, E.N.; Setare, M.R.; Xia, J.Q. Quintom cosmology: Theoretical implications and observations. *Phys. Rep.* **2010**, *493*, 1–60.
41. Nojiri, S.I.; Odintsov, S.D. Final state and thermodynamics of a dark energy universe. *Phys. Rev.* **2004**, *70*, 103522. [CrossRef]
42. Guo, Z.K.; Piao, Y.S.; Zhang, X.; Zhang, Y.Z. Cosmological evolution of a quintom model of dark energy. *Phys. Lett.* **2005**, *608*, 177–182. [CrossRef]
43. Cai, Y.F.; Li, M.; Lu, J.X.; Piao, Y.S.; Qiu, T.; Zhang, X. A string-inspired quintom model of dark energy. *Phys. Lett.* **2007**, *651*, 1–7. [CrossRef]
44. Zhao, G.B.; Xia, J.Q.; Li, M.; Feng, B.; Zhang, X. Perturbations of the quintom models of dark energy and the effects on observations. *Phys. Rev.* **2005**, *72*, 123515. [CrossRef]
45. Feng, B.; Li, M.; Piao, Y.S.; Zhang, X. Oscillating quintom and the recurrent universe. *Phys. Lett.* **2006**, *634*, 101–105. [CrossRef]
46. Bagla, J.S.; Jassal, H.K.; Padmanabhan, T. Cosmology with tachyon field as dark energy. *Phys. Rev.* **2003**, *67*, 063504. [CrossRef]
47. Setare, M.R.; Sadeghi, J.; Amani, A.R. Interacting tachyon dark energy in non-flat universe. *Phys. Lett.* **2009**, *673*, 241–246. [CrossRef]
48. Copeland; E.J.; Garousi, M.R.; Sami, M.; Tsujikawa, S. What is needed of a tachyon if it is to be the dark energy? *Phys. Rev.* **2005**, *71*, 043003. [CrossRef]
49. Wei, H.; Cai, R.G.; Zeng, D.F. Hessence: A new view of quintom dark energy. *Class. Quantum Gravity* **2005**, *22*, 3189. [CrossRef]
50. Alimohammadi, M.; Sadjadi, H.M. Attractor solutions for general hessence dark energy. *Phys. Rev.* **2010**, *73*, 83527. [CrossRef]
51. Chimento, L.P. Extended tachyon field, Chaplygin gas, and solvable k-essence cosmologies. *Phys. Rev.* **2004**, *69*, 123517.
52. Gorini, V.; Kamenshchik, A.; Moschella, U.; Pasquier, V. The Chaplygin gas as a model for dark energy. In *The Tenth Marcel Grossmann Meeting: On Recent Developments in Theoretical and Experimental General Relativity, Gravitation and Relativistic Field Theories (In 3 Volumes)*; World Scientific: Singapore, 2005; pp. 840–859.
53. Setare, M.R. Interacting holographic generalized Chaplygin gas model. *Phys. Lett. B* **2007**, *654*, 1–6. [CrossRef]
54. Setare, M.R. Holographic Chaplygin gas model. *Phys. Lett. B* **2007**, *648*, 329–332. [CrossRef]
55. Avelino, P.P.; Bolejko, K.; Lewis, G.F. Nonlinear Chaplygin gas cosmologies. *Phys. Rev. D* **2014**, *89*, 103004. [CrossRef]
56. Zhang, H.; Zhu, Z.H. Interacting chaplygin gas. *Phys. Rev. D* **2006**, *73*, 043518. [CrossRef]
57. Li, M. A model of holographic dark energy. *Phys. Lett. B* **2004**, *603*, 1–5. [CrossRef]

58. Jamil, M.; Saridakis, E.N.; Setare, M.R. Holographic dark energy with varying gravitational constant. *Phys. Lett.* **2009**, *679*, 172–176. [CrossRef]
59. Nojiri, S.I.; Odintsov, S.D.; Paul, T. Different faces of generalized holographic dark energy. *Symmetry* **2021**, *13*, 928. [CrossRef]
60. Bamba, K.; Capozziello, S.; Nojiri, S.I.; Odintsov, S.D. Dark energy cosmology: The equivalent description via different theoretical models and cosmography tests. *Astrophys. Space Sci.* **2012**, *342*, 155–228. [CrossRef]
61. Elizalde, E.; Nojiri, S.I.; Odintsov, S.D.; Wang, P. Dark energy: Vacuum fluctuations, the effective phantom phase, and holography. *Phys. Rev.* **2005**, *71*, 103504. [CrossRef]
62. Ghosh, R.; Pasqua, A.; Chattopadhyay, S. Generalized second law of thermodynamics in the emergent universe for some viable models of f (T) gravity. *Eur. Phys. J. Plus* **2013**, *128*, 1–11. [CrossRef]
63. Saridakis, E.N.; Basilakos, S. The generalized second law of thermodynamics with Barrow entropy. *Eur. Phys. J.* **2021**, *81*, 1–6. [CrossRef]
64. Singh, C.P.; Kumar, A. Viscous Ricci dark energy and generalized second law of thermodynamics in modified f (R, T) gravity. *Mod. Phys. Lett.* **2018**, *33*, 1850225. [CrossRef]
65. Benaoum, H. Accelerated universe from modified Chaplygin gas and tachyonic fluid. *Universe* **2022**, *8*, 340. [CrossRef]
66. Polarski, D. Dark energy. *Int. J. Mod. Phys. D* **2013**, *22*, 1330027 [CrossRef]
67. Straumann, N. Dark energy: Recent developments. *Mod. Phys. Lett. A* **2006**, *21*, 1083–1098. [CrossRef]
68. Yoo, J.; Watanabe, Y. Theoretical models of dark energy. *Int. J. Mod. Phys. D* **2006**, *21*, 1230002 [CrossRef]
69. Sahni, V.; Starobinsky, A. Reconstructing dark energy. *Int. J. Mod. Phys. D* **2006**, *15*, 2105–2132. [CrossRef]
70. Sahni, V.; Shafieloo, A.; Starobinsky, A.A. Model-independent evidence for dark energy evolution from baryon acoustic oscillations. *Astrophys. J. Lett.* **2014**, *793*, L40. [CrossRef]
71. Spergel, D.N.; Steinhardt, P.J. Observational evidence for self-interacting cold dark matter. *Phys. Rev. Lett.* **2000**, *84*, 3760. [CrossRef]
72. Liddle, A.R.; Lyth, D.H. The Cold dark matter density perturbation. *Phys. Rep.* **1993**, *231*, 1–105. [CrossRef]
73. Amendola, L.; Finelli, F.; Burigana, C.; Carturan, D. WMAP and the generalized Chaplygin gas. *J. Cosmol. Astropart. Phys.* **2003**, *2003*, 5. [CrossRef]
74. Bilić, N.; Tupper, G.B.; Viollier, R.D. Unification of dark matter and dark energy: The inhomogeneous Chaplygin gas. *Phys. Lett. B* **2002**, *535*, 17–21. [CrossRef]
75. Gorini, V.; Kamenshchik, A.; Moschella, U. Can the Chaplygin gas be a plausible model for dark energy? *Phys. Rev.* **2003**, *67*, 063509. [CrossRef]
76. Sahni, V. Dark matter and dark energy. *arXiv*, **2004**, arXiv:0403324.
77. Sen, A.A.; Scherrer, R.J. Generalizing the generalized Chaplygin gas. *Phys. Rev.* **2005**, *72*, 063511. [CrossRef]
78. Kamenshchik, A.; Moschella, U.; Pasquier, V. An alternative to quintessence. *Phys. Lett.* **2001**, *511*, 265–268. [CrossRef]
79. Bento, M.C.; Bertolami, O.; Sen, A. Generalized Chaplygin gas, accelerated expansion and dark Energy-Matter unification. *Phys. Rev. D* **2002**, *66*, 043507. [CrossRef]
80. Pun, C.S.J.; Gergely, L.; Mak, M.K.; Kovcs, Z.; Szab, G.M.; Harko, T. Viscous dissipative Chaplygin gas dominated homogenous and isotropic cosmological models. *Phys. Rev. D* **2008**, *77*, 063528. [CrossRef]
81. Thakur, P.; Ghose, S.; Paul, B.C. Modified Chaplygin gas and constraints on its B parameter from cold dark matter and unified dark matter energy cosmological models. *Mon. Not. R. Astron. Soc.* **2009**, *397*, 1935–1939. [CrossRef]
82. Pourhassan, B. Viscous modified cosmic Chaplygin gas cosmology. *Int. J. Mod. Phys.* **2013**, *22*, 1350061. [CrossRef]
83. Chattopadhyay, S. Modified Chaplygin gas equation of state on viscous dissipative extended holographic Ricci dark energy and the cosmological consequences. *Int. J. Mod. Phys.* **2017**, *26*, 1750042. [CrossRef]
84. Jawad, A.; Ilyas, A.; Rani, S. Dynamics of modified Chaplygin gas inflation on the Brane with bulk viscous pressure. *Int. J. Mod. Phys. D* **2017**, *26*, 1750031. [CrossRef]
85. Bedran, M.L.; Soares, V.; Araujo, M.E. Temperature evolution of the FRW universe filled with modified Chaplygin gas. *Phys. Lett.* **2008**, *659*, 462–465. [CrossRef]
86. Panigrahi, D.; Chatterjee, S. Thermodynamics of the variable modified Chaplygin gas. *J. Cosmol. Astropart. Phys.* **2016**, *2016*, 52. [CrossRef]
87. Salti, M.; Kangal, E.E.; Aydogdu, O. Variable polytropic gas cosmology. *Ann. Phys.* **2019**, *407*, 166–178. [CrossRef]
88. Kamenshchik, A.Y.; Tronconi, A.; Venturi, G. Reconstruction of scalar potentials in induced gravity and cosmology. *Phys. Lett.* **2011**, *702*, 191–196. [CrossRef]
89. Gorbunov, D.S.; Rubakov, V.A. *Introduction to the Theory of the Early Universe: Cosmological Perturbations and Inflationary Theory*; World Scientific: Singapore, 2011.
90. Odintsov, S.D.; Oikonomou, V.K. Deformed matter bounce with dark energy epoch. *Phys. Rev.* **2016**, *94*, 064022. [CrossRef]
91. Nojiri, S.; Odintsov, S. Modified gravity with negative and positive powers of the curvature: Unification of the inflation and of the cosmic acceleration Phys. *arXiv* **2003**, arXiv:hep-th/0307288.
92. Capozziello, S.; Nojiri, S.I.; Odintsov, S.D. Unified phantom cosmology: Inflation, dark energy and dark matter under the same standard. *Phys. Lett.* **2006**, *632*, 597–604. [CrossRef]
93. Huang, Q.G.; Li, M. The holographic dark energy in a non-flat universe. *J. Cosmol. Astropart. Phys.* **2004**, *2004*, 13. [CrossRef]

94. Wang, B.; Gong, Y.; Abdalla, E. Transition of the dark energy equation of state in an interacting holographic dark energy model. *Phys. Lett.* **2005**, *624*, 141–146. [CrossRef]
95. Cai, Y.F. Exploring bouncing cosmologies with cosmological surveys. *Sci. China Phys. Mech. Astron.* **2014**, *57*, 1414–1430. [CrossRef]
96. Lehners, J.L. Ekpyrotic and cyclic cosmology. *Phys. Rep.* **2008**, *465*, 223–263. [CrossRef]
97. Odintsov, S.D.; Oikonomou, V.K. Bouncing cosmology with future singularity from modified gravity. *Phys. Rev.* **2015**, *92*, 024016. [CrossRef]
98. Bamba, K.; Makarenko, A.N.; Myagky, A.N.; Nojiri, S.I.; Odintsov, S.D. Bounce cosmology from F (R) gravity and F (R) bigravity. *J. Cosmol. Astropart. Phys.* **2014**, *2014*, 8. [CrossRef]
99. Bamba, K.; Odintsov, S.D. Inflationary cosmology in modified gravity theories. *Symmetry* **2015**, *7*, 220–240. [CrossRef]
100. Chattopadhyay, S. A study on the bouncing behavior of modified Chaplygin gas in presence of bulk viscosity and its consequences in the modified gravity framework. *Int. J. Geom. Methods Mod. Phys.* **2017**, *14*, 1750181. [CrossRef]
101. Elizalde, E.; Nojiri, S.I.; Odintsov, S.D.; Sáez-Gómez, D.; Faraoni, V. Reconstructing the universe history, from inflation to acceleration, with phantom and canonical scalar fields. *Phys. Rev.* **2008**, *77*, 106005. [CrossRef]
102. Odintsov, S.D.; Paul, T. Bounce universe with finite-time singularity. *Universe* **2022**, *8*, 292. [CrossRef]
103. Nojiri, S.I.; Odintsov, S.D.; Paul, T. Towards a smooth unification from an ekpyrotic bounce to the dark energy era. *Phys. Dark Universe* **2022**, *35*, 100984. [CrossRef]
104. Pourhassan, B. Unified universe history through phantom extended Chaplygin gas. *Can. J. Phys.* **2016**, *94*, 659–670. [CrossRef]
105. Brevik, I.; Timoshkin, A.V. Viscous fluid holographic bounce. *Int. J. Geom. Methods Mod. Phys.* **2020**, *17*, 2050023. [CrossRef]
106. Nojiri, S.; Odintsov, S.D.; Oikonomou, V.K. Quantitative analysis of singular inflation with scalar-tensor and modified gravity. *Phys. Rev.* **2015**, *91*, 84059. [CrossRef]
107. Nojiri, S.; Odintsov, S.D.; Oikonomou, V.K. Singular inflation from generalized equation of state fluids. *Phys. Lett.* **2015**, *747*, 310–320. [CrossRef]
108. Odintsov, S.D.; Oikonomou, V.K.; Timoshkin, A.V.; Saridakis, E.N.; Myrzakulov, R. Cosmological fluids with logarithmic equation of state. *Ann. Phys.* **2018**, *398*, 238–253. [CrossRef]
109. Weinberg, S. Entropy generation and the survival of protogalaxies in an expanding universe. *Astrophys. J.* **1971**, *168*, 175. [CrossRef]
110. Hassani, H.; Soofi, A.S.; Zhigljavsky, A. Predicting inflation dynamics with singular spectrum analysis. *J. R. Stat. Soc., A: Stat. Soc.* **2013**, *176*, 743–760. [CrossRef]
111. Armendariz-Picon, C.; Greene, P.B. Spinors, inflation, and non-singular cyclic cosmologies. *Gen Relativ Gravit* **2003**, *35*, 1637–1658. [CrossRef]
112. Biswas, T.; Mazumdar, A. Super-inflation, non-singular bounce, and low multipoles. *Class. Quantum Gravity* **2013**, *31*, 025019. [CrossRef]
113. Aziza, A.; Chakraborty, G.; Chattopadhyay, S. Variable generalized Chaplygin gas in f (Q) gravity and the inflationary cosmology. *Int. J. Mod. Phys. D* **2021**, *30*, 2150119. [CrossRef]
114. Brevik, I.; Nojiri, S.I.; Odintsov, S.D.; Vanzo, L. Entropy and universality of the Cardy-Verlinde formula in a dark energy universe. *Phys. Rev.* **2004**, *70*, 43520. [CrossRef]
115. Cardone, V.F.; Troisi, A.; Capozziello, S. Phenomenological model for inflationary quintessence. *Phys. Rev.* **2005**, *72*, 43501. [CrossRef]
116. Zimdahl, W. Bulk viscous cosmology. *Phys. Rev.* **1996**, *53*, 5483. [CrossRef]
117. Clifton, T.; Ferreira, P.G.; Padilla, A.; Skordis, C. Modified gravity and cosmology. *Phys. Rep.* **2021**, *513*, 1–189. [CrossRef]
118. Nojiri, S.I.; Odintsov, S.D. Introduction to modified gravity and gravitational alternative for dark energy. *Int. J. Geom. Methods Mod. Phys.* **2007**, *4*, 115–145. [CrossRef]
119. Tsujikawa, S. Modified gravity models of dark energy. In *Lectures on Cosmology: Accelerated Expansion of the Universe*; Springer: Berlin/Heidelberg, Germany, 2010; pp. 99–145.
120. Chattopadhyay, S. Cosmological bounce in a modified gravity framework. *Astron. Nachrichten* **2023**, *344*, 220103. [CrossRef]
121. Barros, B.J.; Teixeira, E.M.; Vernieri, D. Bouncing cosmology in f (R, G) gravity by order reduction. *Ann. Phys.* **2020**, *419*,168231. [CrossRef]
122. Biswas, T.; Mazumdar, A.; Siegel, W. Bouncing universes in string-inspired gravity. *J. Cosmol. Astropart. Phys.* **2006**, *03*, 009. [CrossRef]
123. Makarenko, A.N.; Myagky, A.N. The asymptotic behavior of bouncing cosmological models in F(G) gravity theory. *Int. J. Geom. Methods Mod. Phys.* **2017**, *14*, 1750148. [CrossRef]
124. Bertschinger, E.; Zukin, P. Distinguishing modified gravity from dark energy. *Phys. Rev.* **2008**, *78*, 024015. [CrossRef]
125. de Cesare, M. Reconstruction of mimetic gravity in a non-singular bouncing universe from quantum gravity. *Universe* **2019**, *5*, 107. [CrossRef]
126. Capozziello, S.; Matsumoto, J.; Nojiri, S.I.; Odintsov, S.D. Dark energy from modified gravity with Lagrange multipliers. *Phys. Lett.* **2010**, *693*, 198–208. [CrossRef]
127. Hu, W.; Sawicki, I. Parametrized post-Friedmann framework for modified gravity. *Phys. Rev.* **2007**, *76*, 104043. [CrossRef]

128. Nojiri, S.I.; Odintsov, S.D. Modified gravity and its reconstruction from the universe expansion history. *J. Physics Conf. Ser.* ***2007***, *66*, *012005.* [CrossRef]
129. Shtanov, Y.; Sahni, V. Bouncing braneworlds. *Phys. Lett. B* **2017**, *557*, 1–6. [CrossRef]
130. Alesci, E.; Botta, G.; Cianfrani, F.; Liberati, S. Cosmological singularity resolution from quantum gravity: The emergent-bouncing universe. *Phys. Rev. D* **2017**, *96*, 046008. [CrossRef]
131. Millano, A.D.; Jusufi, K.; Leon, G. Phase space analysis of the bouncing universe with stringy effects. *Phys. Lett. B* **2023**, *841*, 137916. [CrossRef]
132. Shamir, M.F. Bouncing universe in f (G, T) gravity. *Phys. Dark Universe* **2021**, *32*, 100794. [CrossRef]
133. Saha, S.; Chattopadhyay, S. Viscous generalised Chaplygin gas under the purview of f(T) gravity and the model assessment through probabilistic information theory. *Phys. Scr.* **2020**, *97*, 045006. [CrossRef]
134. Ganguly, C.; Quintin, J. Microphysical manifestations of viscosity and consequences for anisotropies in the very early universe. *Phys. Rev.* **2022**, *105*, 023532. [CrossRef]
135. Barrow, J.D.; Graham, A.A. Singular inflation. *Phys. Rev.* **2015**, *91*, 83513. [CrossRef]
136. Cai, Y.-F.; Chen, S.-H.; Dent, J.B.; Dutta, S.; Saridakis, E.N. Matter bounce cosmology with the f(T) gravity. *Class. Quantum Gravity* **2011**, *28*, 215011. [CrossRef]
137. Nojiri, S.I.; Odintsov, S.D.; Saridakis, E.N. Holographic inflation. *Phys. Lett.* **2019**, *797*, 134829. [CrossRef]
138. Bento, M.D.C.; Bertolami, O.; Sen, A.A. Generalized Chaplygin gas and cosmic microwave background radiation constraints. *Phys. Rev.* **2003**, *67*, 063003. [CrossRef]
139. Tsujikawa, S.; Sami, M. A unified approach to scaling solutions in a general cosmological background. *Phys. Lett. B* **2004**, *603*, 113–123. [CrossRef]
140. Ranjit, C.; Islam, S.; Chattopadhyay, S.; Gudekli, E. Analysis of different scenarios with new Tsallis holographic dark energies and bulk viscous fluid in the framework of Chern–Simons modified gravity. *Int. J. Mod. Phys. E* **2021**, 36, 2150151. [CrossRef]
141. Karmakar, S.; Myrzakulov, K.; Chattopadhyay, S.; Myrzakulov, R. Reconstructed f (R) Gravity and Its Cosmological Consequences in theChameleon Scalar Field with a Scale Factor Describing the Pre-Bounce Ekpyrotic Contraction. *Symmetry* **2020**, *12*, 1559. [CrossRef]
142. Nojiri, S.I.; Odintsov, S.D.; Paul, T. Early and late universe holographic cosmology from a new generalized entropy. *Phys. Rev. B* **2022**, *831*, 137189. [CrossRef]
143. Ijjas, A.; Steinhardt, P.J. Classically stable nonsingular cosmological bounces. *Phys. Rev. Lett.* **2016**, *117*, 121304. [CrossRef]
144. Boruah, S.S.; Kim, H.J.; Rouben, M.; Geshnizjani, G. Cuscuton bounce. *JCAP* **2018**, *08*, 031. [CrossRef]
145. Ijjas, A.; Ripley, J.; Steinhardt, P.J. NEC violation in mimetic cosmology revisited. *Phys. Lett. B* **2016**, *760*, 132–138. [CrossRef]
146. C de Rham, C.; Melville, S. Unitary null energy condition violation in P (X) cosmologies. *Phys. Rev. D* **2017**, *95*, 123523. [CrossRef]
147. Agrawal, A.S.; Mishra, S.; Tripathy, S.K.; Mishra, B. Bouncing cosmological models in the functional form of F (R) gravity. *arXiv* **2022**, arXiv:2210.09726.
148. Ahmed, N.; Kamel, T.M.; Nouh, M.I. A non-singular closed bouncing universe without violation of null energy condition. *arXiv* **2022**, arXiv:2204.11854.
149. Visser, M. Cosmography: Cosmology without the Einstein equations. *Gen Relativ Gravit.* **2005**, *37*, 1541–1548. [CrossRef]
150. Tripathy, S.K.; Khuntia, R.K.; Parida, P. Bouncing cosmology in an extended theory of gravity. *Eur. Phys. J. Plus* **2019**, *134*, 1–13.
151. Singh, J.K.; Bamba, K.; Nagpal, R.; Pacif, S.K.J. Bouncing cosmology in f (R, T) gravity. *Phys. Rev. D* **2018**, *97*, 123536. [CrossRef]
152. Chakraborty, S.; Gregoris, D. Cosmological evolution with quadratic gravity and nonideal fluids. *Eur. Phys. J. C* **2021**, *81*, 1–30. [CrossRef]
153. Hoffman, M.B.; Turner, M.S. Kinematic constraints to the key inflationary observables. *Phys. Rev. D* **2001**, *64*, 023506 [CrossRef]
154. Coone, D.; Roesta, D.; Venninc, V. The Hubble flow of plateau inflation. *J. Cosmol. Astrophys.* **2015**, *1511*, 010. [CrossRef]
155. Odintsov, S.D.; Oikonomou, V.K. Singular inflationary universe from F (R) gravity. *Phys. Rev. D* **2015**, *92*, 124024. [CrossRef]
156. Bhattacharjee, S.; Sahoo, P.K. Comprehensive analysis of a non-singular bounce in f (R, T) gravitation. *Phys. Dark Universe.* **2020**, *28*, 100537. [CrossRef]
157. Ganiou, M.G.; Houndjo, M.J.S.; Aïnamon, C.; Ayivi, L.; Kanfon, A. Reconstruction method applied to bounce cosmology and inflationary scenarios in cosmological f (G) gravity. *Eur. Phys. J. Plus* **2022**, *137*, 208. [CrossRef]
158. Paul, T.; SenGupta, S. Ekpyrotic bounce driven by Kalb–Ramond field. *Phys. Dark Universe* **2023**, *41*, 101236. [CrossRef]
159. Nojiri, S.; Odintsov, S.D.; Oikonomou, V. Modified gravity theories on a nutshell: Inflation, bounce and late-time evolution. *Phys. Rep.* **2017**, *692*, 1–104. [CrossRef]
160. Lam, Y.M.P. Perturbation Lagrangian theory for scalar fields-Ward-Takahashi identity and current algebra. *Phys. Rev.* **1972**, *6*, 2145. [CrossRef]
161. Nojiri, S.I.; Odintsov, S.D. Unifying phantom inflation with late-time acceleration: Scalar phantom–non-phantom transition model and generalized holographic dark energy. *Gen. Relativ. Gravit.* **2006**, *38*, 1285–1304 [CrossRef]
162. Biswas, T.; Koshelev, A.S.; Mazumdar, A.; Vernov, S.Y. Stable bounce and inflation in non-local higher derivative cosmology. *J. Cosmol. Astropart. Phys.* **2012**, *08*, 024. [CrossRef]
163. Brandenberger, R.H. The matter bounce alternative to inflationary cosmology. *arXiv*, **2012** arXiv:1206.4196.
164. Silva, W.C.E.; Shapiro, I.L. Bounce and stability in the early cosmology with anomaly-induced corrections. *Symmetry* **2020**, *13*, 50. [CrossRef]

165. Linsefors, L.; Barrau, A. Duration of inflation and conditions at the bounce as a prediction of effective isotropic loop quantum cosmology. *Phys. Rev. D* **2013**, *87*, 123509. [CrossRef]
166. Ijjas, A.; Steinhardt, P.J. Implications of Planck2015 for inflationary, ekpyrotic and anamorphic bouncing cosmologies. *Class. Quantum Gravity* **2016**, *33*, 044001. [CrossRef]
167. Nojiri, S.I.; Odintsov, S.D. Covariant generalized holographic dark energy and accelerating universe. *Eur. Phys. J.* **2017**, *77*, 528. [CrossRef]
168. Brevik, I.; Grøn, Ø.; de Haro, J.; Odintsov, S.D.; Saridakis, E.N. Viscous cosmology for early-and late-time universe. *Int. J. Mod. Phys.* **2017**, *26*, 1730024. [CrossRef]
169. Billyard, A.P.; Coley, A.A. Interactions in scalar field cosmology. *Phys. Rev.* **2000**, *61*, 083503. [CrossRef]
170. Chervon, S.V.; Fomin, I.V.; Beesham, A. The method of generating functions in exact scalar field inflationary cosmology. *Eur. Phys. J.* **2018**, *78*, 301 [CrossRef]
171. Barrow, J.D.; Saich, P. Scalar-field cosmologies. *Class. Quantum Gravity* **1993**, *10*, 279. [CrossRef]